NASA CONTRACTOR
REPORT

NASA CR-2088

A STUDY OF RADIOMETRIC EMISSION
FROM A ROUGH SEA SURFACE

by A. Stogryn

Prepared by
MICROWAVE DIVISION
AEROJET-GENERAL CORPORATION
El Monte, Calif. 91734
for Langley Research Center

NATIONAL AERONAUTICS AND SPACE ADMINISTRATION • WASHINGTON, D. C. • JULY 1972

0061170

1. Report No. NASA CR-2088	2. Government Accession No.	3. Recipient's Catalog No.
4. Title and Subtitle A STUDY OF RADIOMETRIC EMISSION FROM A ROUGH SEA SURFACE		5. Report Date July 1972
		6. Performing Organization Code
7. Author(s) A. Stogryn		8. Performing Organization Report No. 3000R - 1
		10. Work Unit No.
9. Performing Organization Name and Address Aerojet-General Corporation Microwave Division 9200 East Flair Drive El Monte, California 91734		
		11. Contract or Grant No. NAS 1-10633
		13. Type of Report and Period Covered Contractor Report
12. Sponsoring Agency Name and Address National Aeronautics and Space Administration Washington, D.C. 20546		
		14. Sponsoring Agency Code

15. Supplementary Notes

16. Abstract

    The equation which describe the emissivity of a rough ocean surface are developed.
The theory includes effects of large scale and small scale wave structure and the influence
of shadowing by the large ocean waves. Also included are investigations of the emission
properties of foam and the influence of the thermal boundary layer on the brightness
temperature characteristics of the ocean surface.

17. Key Words (Suggested by Author(s)) Electromagnetic scattering from rough surfaces Microwave emission from the ocean Emissivity of sea foam Thermal radiation from the ocean		18. Distribution Statement Unclassified - Unlimited		
19. Security Classif. (of this report) Unclassified	20. Security Classif. (of this page) Unclassified		21. No. of Pages 80	22. Price* $3.00

*For sale by the National Technical Information Service, Springfield, Virginia 22151

FOREWORD

This document is the final technical report summarizing research performed by the Microwave Division of Aerojet-General Corporation for the National Aeronautics and Space Administration, Langley Research Center, Hampton, Virginia under Contract NAS 1-10633.

The objective of the program was to broaden the understanding of the microwave radiometric emission characteristics of the ocean. The principal problems which were investigated were the following:

a.   The microwave emission properties of foam on the ocean's surface.

b.   The influence of the ocean's thermal boundary layer on its brightness temperature characteristics.

c.   A study of the influence of ocean waves which included shadowing and the effects of the small scale wave structure of the ocean.

Complete, self-contained reports covering the work accomplished under Items a. and b. were issued on April 30, 1971 and May 20, 1971 respectively. However, for completeness, these documents are reproduced as Appendixes A and B in the present report. The contractor was also granted permission to publish the report on the properties of sea foam in the standard scientific literature. This paper has been accepted and will shortly be published in the Journal of Geophysical Research.

The remainder of the present report discusses studies relating to Item c. and also shows some numerical results which have been obtained. The development of the theory relating to Item c. is complete and is discussed in the section of this report entitled "The Effect of Waves on the Microwave Brightness Temperature of the Sea." It was intended to be and may be read as an independent and self-contained document.

Numerical results using the complete theory developed for wave effects and foam have, unfortunately, not been obtained yet. However partial results including the effects of the large scale structure, shadowing,

and foam have been obtained and are discussed in the section entitled "The Brightness Temperature of the Sea." Comparison of the numerical results with published data at 19.4 GHz indicates that substantial progress has been made in the description of the microwave radiometric characteristics of the ocean. It is to be hoped that further computations which include the effects of the small scale structure of the sea surface will lead to a similar close agreement between theory and experiment at lower frequencies.

CONTENTS

ILLUSTRATIONS

Section 1

THE EFFECT OF WAVES ON THE MICROWAVE
BRIGHTNESS TEMPERATURE OF THE SEA

1.1   INTRODUCTION

The problem of describing the microwave emission characteristics of the sea has recently received considerable attention in view of its potential application to oceanography and meteorology. Since the publication of a theoretical study by Stogryn (Ref. 1) on the effects of waves, a number of experiments relating to this problem have been reported in the established literature (Refs. 2 through 6) as well as in documents receiving more limited distribution. Although some experiments (Refs. 2 and 3) appear to provide a partial verification of the predictions in Reference 1, others (Refs. 4, 5 and 6) produced results at variance with the theory. An examination of his data resulted in the suggestion by Williams (Ref. 6) that foam on the water's surface plays a significant part in the emission properties of the sea. With the adoption of this hypothesis, it is immediately clear why apparently discrepant results have been obtained. The properties of foam (Refs. 7 and 8) are much different from water in bulk form so that those data (Refs. 4 through 6) which refer to a sea surface with both waves and foam must be analyzed using a theory which accounts separately for the emission effects of foam (weighted with respect to the percentage foam cover) and the emission effects of waves. Both effects are important and have different ranges where they predominate. To achieve an adequate understanding of the factors involved, it is apparent that theory and experiments which provide data separately on foam and on waves must be compared.

It is the intent of this work to extend the theory of wave effects given in Reference 1 with a view toward explaining some observed features of sea surface emission which are not adequately accounted for using an emission theory based solely on the Kirchhoff approximation. A two-scale model for describing the roughness characteristics of the sea surface, treating the large waves differently from the small scale ripples, is developed.

Foam effects are explicitly excluded from consideration. The theory may ultimately be compared with the data of Hollinger (Refs. 2 and 3), who systematically excluded foam patches from his observations.

1.2 THE TWO-SCALE MODEL

Peake (Ref. 9) has shown how the thermal emission and reflection properties of a surface may be related to a set of scattering coefficients $\gamma_{ab}(\hat{k}_o, \hat{k})$ defined as

$$\gamma_{ab}(\hat{k}_o, \hat{k}) = \lim_{A \to \infty} \lim_{R \to \infty} \frac{4\pi R^2}{A \cos\theta_o} \frac{(I_s)_b}{(I_o)_a} \tag{1-1}$$

where $(I_o)_a$ is the intensity of radiation with polarization described by a unit vector $\hat{a}$ incident from a direction described by the unit propagation vector $\hat{k}_o$ on a rough surface S whose projection on the x-y plane is A, and $(I_s)_b$ is the intensity of the radiation scattered in the direction of the unit propagation vector $\hat{k}$ and polarization $\hat{b}$ at a distance R from S. The relevant geometry is illustrated in Figure 1. As is customary in radiometric studies, the polarization directions will be taken to be either horizontal $(\hat{h})$ or vertical $(\hat{v})$ in this work.
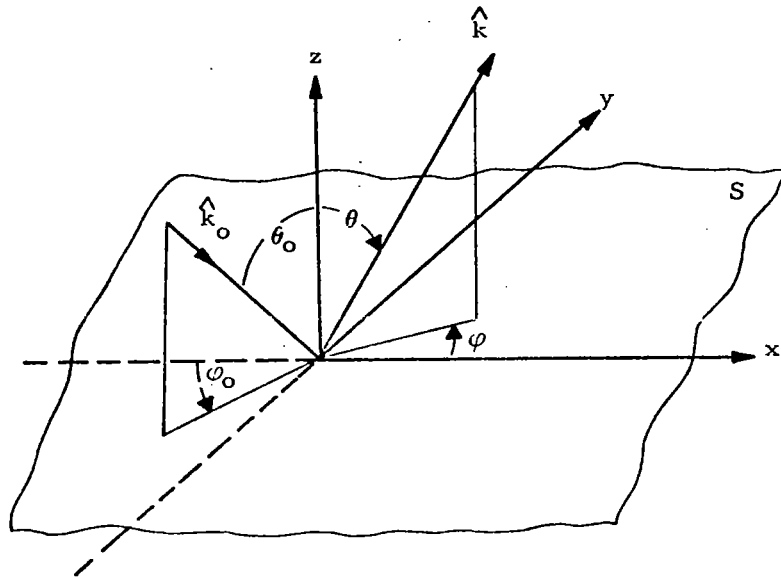

Figure 1. Scattering Geometry

In Reference 1, estimates for the brightness temperature due to ocean waves were given on the basis of the Kirchhoff approximation for γ_{ab}. However, the Kirchhoff approximation is expected to be good only for surfaces whose slope is not too great and whose radii of curvature are large compared to the electromagnetic wavelength. In application to the ocean, this condition is met by the large gravity waves, but the effects of small ripples on the water's surface would not be treated properly at microwave frequencies. Thus, an extension of the model is desirable. This may be achieved by considering the ocean's surface to consist of a surface whose roughness scale is small compared to the electromagnetic wavelength (the ripples) and which rides on top of the large gravity waves. Scattering from the ripples may be treated by means of small perturbation theory while the effects of the large scale structure may be treated by an appropriate geometrical optics method. Such an approach requires a somewhat arbitrary division of the true surface into two components which does not have a strong physical basis from the point of view of oceanography. However, from the electromagnetic standpoint, there is a range of water wavelengths and heights where either the Kirchhoff approximation or a treatment based on perturbation theory should be valid. Hence, there exists some latitude for the separation into two components so that the exact point of division should not play a critical role. It should be noted here that such a two-scale approach has led to useful results in interpreting radar backscattering data from certain kinds of surfaces.

Upon accepting this model, the problem of computing the total scattering coefficients arises. To do this, assume that the large scale roughness may be represented locally by a plane with unit normal $\hat{n}$ and that the scattering characteristics of the small scale structure are known. The scattering coefficients relative to the inclined surface surface whose mean plane has normal $\hat{n}$ are

$$\gamma_{ab}(\hat{n}, \hat{k}_o, \hat{k}) = \frac{4\pi R^2}{A_n(-\hat{k}_o \cdot \hat{n})} \frac{(I_s)_b}{(I_o)_a} \qquad (1\text{-}2)$$

3

where A_n is the projection of the surface under consideration (representing the small scale roughness) on the inclined plane and, for convenience, the limit signs in definition (1-1) have been omitted. Since an average over the normal directions will eventually be required, it is necessary to reference all quantities to the mean sea surface whose normal is the unit vector $\hat{z}$. Relative to the reference plane, the inclined surface has scattering coefficients

$$\gamma_{ab}(\hat{z}, \hat{k}_o, \hat{k}) = \frac{4\pi R^2}{A(-\hat{k}_o \cdot \hat{z})} \frac{(I_s)_b}{(I_o)_a} \tag{1-3}$$

But $A = A_n(\hat{n} \cdot \hat{z})$ so that (1-3) may be expressed as

$$\gamma_{ab}(\hat{z}, \hat{k}_o, \hat{k}) = \gamma_{ab}(\hat{n}, \hat{k}, \hat{k}_o) \frac{\hat{k}_o \cdot \hat{n}}{(\hat{n} \cdot \hat{z})(\hat{k}_o \cdot \hat{z})} \tag{1-4}$$

Now, the scattering coefficients of the sea are obtained by averaging (1-4) over the slope spectrum of the large scale structure. A refinement may be introduced by realizing that only part of the sea surface will be illuminated by an incoming wave with direction $\hat{k}_o$ and that part will be in shadow. Likewise, the scattered wave may strike a portion of the sea surface and thus be shadowed from the direction $\hat{k}$. Thus, the scattering coefficients of the sea may be expressed as

$$\gamma_{ab}(\hat{k}_o, \hat{k}) = \int_{-\infty}^{\infty} \gamma_{ab}(\hat{n}, \hat{k}_o, \hat{k}) \frac{\hat{k}_o \cdot \hat{n}}{(\hat{n} \cdot \hat{z})(\hat{k}_o \cdot \hat{z})} S\, p_T\, d\zeta\, d\zeta_x\, d\zeta_y \tag{1-5}$$

where $p_T\, d\zeta\, d\zeta_x\, d\zeta_y$ is the probability that the large scale structure of the sea has height ζ above the plane $z = 0$ and slopes ζ_x and ζ_y in the x and y directions respectively and S is the probability that neither the incoming nor the scattered wave is in shadow. The vector $\hat{n}$ in (1-5) is related to the slopes ζ_x and ζ_y by

$$\hat{n} = (-\zeta_x, -\zeta_y, 1) \Big/ \sqrt{1 + \zeta_x^2 + \zeta_y^2} \tag{1-6}$$

4

To begin the evaluation of the integrals in (1-5), it will be assumed that the surface height distribution is independent of the slope distribution. Further, the height distribution may be taken to be Gaussian distribution. Thus,

$$p_T(\zeta, \zeta_x, \zeta_y) = p_G(\zeta) \, p(\zeta_x, \zeta_y) \tag{1-7}$$

where p_G is a Gaussian distribution function and p is the slope distribution function for the large scale structure. Shadowing by rough surfaces has been studied by several authors. Although a complete theory is not available, a reasonable approximation for shadowing effects has been found by Sancer (Ref. 10) by using a result of Smith (Ref. 11) for the probability that a line drawn to a given point on the surface will not intersect any other point on the surface. With the assumption that S is simply the product of Smith's probability for the directions $\hat{k}_o$ and $\hat{k}$ (which appears to be a good approximation except for a region where the horizontal component of $\hat{k}$ is nearly equal to the negative of the horizontal component of $\hat{k}_o$), Sancer finds

$$\int_{-\infty}^{\infty} S \, p_G(\zeta) \, d\zeta = \frac{H(-\hat{k}_o \cdot \hat{n}) \; H(\hat{k} \cdot \hat{n})}{1 + \Lambda(\hat{k}_o) + \Lambda(\hat{k})} \tag{1-8}$$

where

$$H(x) = \begin{cases} 0 & \text{if } x < 0 \\ 1 & \text{if } x > 0 \end{cases} \tag{1-9}$$

and

$$\Lambda(\hat{k}) = \frac{1}{2} \left[\frac{\exp(-a^2)}{\sqrt{\pi} \, a} - \mathrm{erfc}(a) \right] \tag{1-10}$$

$$a = \frac{\cot\theta}{\sqrt{2} \left[g_{xL}^2 \cos^2\varphi + g_{yL}^2 \sin^2\varphi \right]} \tag{1-11}$$

In (1-10), erfc is the complementary error function. The angles appearing in (1-11) are shown in Figure 1 while the quantities g_{xL} and g_{yL} are the root-mean-square slopes of the large scale structure in the x and y directions respectively. With these results, (1-5) becomes

$$\gamma_{ab}(\hat{k}_o, \hat{k}) = \int \gamma_{ab}(\hat{n}, \hat{k}_o, \hat{k}) \; \frac{\hat{k}_o \cdot \hat{n} \; H(-\hat{k}_o \cdot \hat{n}) \; H(\hat{k} \cdot \hat{n})}{(\hat{n} \cdot \hat{z})} \; p \; d\zeta_x \; d\zeta_y \Big/$$

$$\Big\{ (\hat{k}_o \cdot \hat{z}) \Big[1 + \Lambda(\hat{k}_o) + \Lambda(\hat{k}) \Big] \Big\} \qquad (1\text{-}12)$$

One further problem relating to (1-12) may be discussed before specialization to a more detailed model is made. The coefficients $\gamma_{ab}(\hat{n}, \hat{k}_o, \hat{k})$ in (1-12) are defined relative to a plane whose normal is $\hat{n}$ and for which the definition of the horizontal and vertical polarization vectors (call these vectors $\hat{H}_o$ and $\hat{V}_o$ for the incident wave directions $\hat{k}_o$, and $\hat{H}$ and $\hat{V}$ for the scattered wave direction $\hat{k}$) does not coincide with $\hat{h}_o$ and $\hat{v}_o$ (the values of a) or $\hat{h}$ and $\hat{v}$ (the values of b) which are defined relative to the plane of the mean sea surface $z = 0$. Hence, it is necessary to obtain transformation equations to the polarization directions appropriate to the mean sea surface. We recall here that, given a plane $\hat{n} \cdot r = 0$ and a propagation vector $\hat{k}$, the horizontal polarization vector with respect to the plane is defined as a unit vector in the direction $\hat{k} \times \hat{n}$ while the vertical polarization vector is defined as $\hat{H} \times \hat{k}$.

Thus, consider a plane electromagnetic wave

$$\underset{\sim}{E}_{inc} = E_o \hat{h}_o \, e^{i \underset{\sim}{k}_o \cdot \underset{\sim}{r}} \qquad (1\text{-}13)$$

of frequency ν with propagation vector $\underset{\sim}{k}_o = \frac{2\pi\nu}{c} \hat{k}_o$ whose polarization is horizontal with respect to the mean sea surface and which is incident on an inclined surface. This field may be decomposed as

$$\underset{\sim}{E}_{inc} = \Big[(\hat{h}_o \cdot \hat{H}_o) \, \hat{H}_o + (\hat{h}_o \cdot \hat{V}_o) \, \hat{V}_o \Big] E_o \, e^{i \underset{\sim}{k}_o \cdot \underset{\sim}{r}} \qquad (1\text{-}14)$$

so that the incident field is expressed as a linear combination of fields polarized in the horizontal and vertical directions with respect to the inclined surface. Therefore, if the surface produces a scattered field $\underset{\sim}{E}_{H_o}$ in the direction $\hat{k}$ in response to an incident field $E_o \hat{H}_o \, e^{i \underset{\sim}{k}_o \cdot \underset{\sim}{r}}$ and a scattered field $\underset{\sim}{E}_{V_o}$ in response to an incident field $E_o \hat{V}_o \, e^{i \underset{\sim}{k}_o \cdot \underset{\sim}{r}}$, the scattered field produced by (1-14) is

$$\underset{\sim}{E}_{h_O} = (\hat{h}_O \cdot \hat{H}_O) \, \underset{\sim}{E}_{H_O} + (\hat{h}_O \cdot \hat{V}_O) \, \underset{\sim}{E}_{V_O} \qquad (1\text{-}15)$$

Hence the $\hat{h}$ and $\hat{v}$ components of the scattered field are

$$\underset{\sim}{E}_{h_O} \cdot \hat{h} = (\hat{h}_O \cdot \hat{H}_O)(\hat{h} \cdot \hat{H}) \, \underset{\sim}{E}_{H_O} \cdot \hat{H} + (\hat{h}_O \cdot \hat{V}_O)(\hat{h} \cdot \hat{H}) \, \underset{\sim}{E}_{V_O} \cdot \hat{H}$$

$$+ (\hat{h}_O \cdot \hat{H}_O)(\hat{h} \cdot \hat{V}) \, \underset{\sim}{E}_{H_O} \cdot \hat{V} + (\hat{h}_O \cdot \hat{V}_O)(\hat{h} \cdot \hat{V}) \, \underset{\sim}{E}_{V_O} \cdot V \qquad (1\text{-}16a)$$

and

$$\underset{\sim}{E}_{h_O} \cdot \hat{v} = (\hat{h}_O \cdot \hat{H}_O)(\hat{v} \cdot \hat{H}) \, \underset{\sim}{E}_{H_O} \cdot \hat{H} + (\hat{h}_O \cdot \hat{V}_O)(\hat{v} \cdot \hat{H}) \, \underset{\sim}{E}_{V_O} \cdot \hat{H}$$

$$+ (\hat{h}_O \cdot \hat{H}_O)(\hat{v} \cdot \hat{V}) \, \underset{\sim}{E}_{H_O} \cdot \hat{V} + (\hat{h}_O \cdot \hat{V}_O)(\hat{v} \cdot \hat{H}) \, \underset{\sim}{E}_{V_O} \cdot \hat{V} \qquad (1\text{-}16b)$$

In a like manner, a vertically polarized plane wave

$$\underset{\sim}{E}_{inc} = E_O \hat{v}_O \, e^{i \underset{\sim}{k}_O \cdot \underset{\sim}{r}} \qquad (1\text{-}17)$$

can be shown to give rise to the scattered field $\underset{\sim}{E}_{v_O}$ with components

$$\underset{\sim}{E}_{v_O} \cdot \hat{h} = (\hat{v}_O \cdot \hat{H}_O)(\hat{h} \cdot \hat{H}) \, \underset{\sim}{E}_{H_O} \cdot \hat{H} + (\hat{v}_O \cdot \hat{V}_O)(\hat{h} \cdot \hat{H}) \, \underset{\sim}{E}_{V_O} \cdot \hat{H}$$

$$+ (\hat{v}_O \cdot \hat{H}_O)(\hat{h} \cdot \hat{V}) \, \underset{\sim}{E}_{H_O} \cdot \hat{V} + (\hat{v}_O \cdot \hat{V}_O)(\hat{v} \cdot \hat{V}) \, \underset{\sim}{E}_{V_O} \cdot \hat{V} \qquad (1\text{-}18a)$$

and

$$\underset{\sim}{E}_{v_O} \cdot \hat{v} = (\hat{v}_O \cdot \hat{H}_O)(\hat{v} \cdot \hat{H}) \, \underset{\sim}{E}_{H_O} \cdot \hat{H} + (\hat{v}_O \cdot \hat{V}_O)(\hat{v} \cdot \hat{H}) \, \underset{\sim}{E}_{V_O} \cdot \hat{H}$$

$$+ (\hat{v}_O \cdot \hat{H}_O)(\hat{v} \cdot \hat{H}) \, \underset{\sim}{E}_{H_O} \cdot \hat{V} + (\hat{v}_O \cdot \hat{V}_O)(\hat{v} \cdot \hat{V}) \, \underset{\sim}{E}_{V_O} \cdot \hat{V} \qquad (1\text{-}18b)$$

Definition (1-1) shows that the scattering coefficients are proportional to $|E_a \cdot \hat{b}|^2$ where a and b may independently assume the values

h or v . Explicit expressions for these coefficients will not be written here because of the large number of terms which are obtained when (1-16) and (1-18) are squared. However, as shown by the analysis of Peake (Ref. 9), the quantities of primary interest in studying the radiometric properties of a surface are not the individual γ_{ab} , but the sums $\gamma_{hh} + \gamma_{hv}$ and $\gamma_{vh} + \gamma_{vv}$. When these quantities are computed, many of the individual terms are seen to cancel if it is observed that since both pairs of vectors $\hat{h}$, $\hat{v}$ and $\hat{H}$, $\hat{V}$ are orthonormal sets perpendicular to $\hat{k}$, the matrix

$$
\begin{pmatrix}
\hat{h} \cdot \hat{H} & \hat{v} \cdot \hat{H} \\
\hat{h} \cdot \hat{V} & \hat{v} \cdot \hat{V}
\end{pmatrix}
$$

is a proper orthogonal matrix. This implies that

$$\hat{h} \cdot \hat{H} = \hat{v} \cdot \hat{V} \tag{1-19a}$$

$$\hat{v} \cdot \hat{H} = -\hat{h} \cdot \hat{V} \tag{1-19b}$$

$$(\hat{h} \cdot \hat{H})^2 + (\hat{h} \cdot \hat{V})^2 = 1 \tag{1-19c}$$

By use of (1-19) and the analog for polarization vectors with subscript o , it is found that

$$\gamma_{hh}(\hat{n}, \hat{k}_o, \hat{k}) + \gamma_{hv}(\hat{n}, \hat{k}_o, \hat{k})$$

$$= (\hat{h}_o \cdot \hat{H})^2 \left[\Gamma_{HH} + \Gamma_{HV} \right] + (\hat{h}_o \cdot \hat{V}_o)^2 \left[\Gamma_{VH} + \Gamma_{VV} \right]$$

$$+ 2(\hat{h}_o \cdot \hat{H}_o)(\hat{h}_o \cdot \hat{V}_o) \left[\Gamma_H + \Gamma_V \right] \tag{1-20a}$$

$$\gamma_{vh}(\hat{n}, \hat{k}_o, \hat{k}) + \gamma_{vv}(\hat{n}, \hat{k}_o, \hat{k})$$

$$= (\hat{h}_o \cdot \hat{V}_o)^2 \left[\Gamma_{HH} + \Gamma_{HV} \right] + (\hat{h}_o \cdot \hat{H}_o)^2 \left[\Gamma_{VH} + \Gamma_{VV} \right]$$

$$- 2(\hat{h}_o \cdot \hat{V}_o)(\hat{h}_o \cdot \hat{H}_o) \left[\Gamma_H + \Gamma_V \right] \tag{1-20b}$$

8

where Γ_{AB} (A, B = H or V) are simply the scattering coefficients defined by Peake for the small scale structure of the sea. It will be noted, however, that two new quantities which are defined as

$$\Gamma_B = \frac{4\pi R^2}{E_o^2 A_n(-\hat{k}_o \cdot \hat{n})} \; \text{Re}\left[\left(\underset{\sim}{E}_{H_o} \cdot \hat{B}\right)\left(\underset{\sim}{E}^*_{V_o} \cdot \hat{B}\right)\right] \tag{1-21}$$

are required (compare with definition (1-2)). In (1-21), Re means "real part of" and the asterisk indicates complex conjugate. These additional terms arise solely because of the tilt of the plane carrying the small scale structure.

With the substitution of (1-20) into the appropriate sums of terms shown in (1-12), the analysis has been carried to a point which requires explicit expressions for the scattering coefficients appearing in the integrals.

1.3   SCATTERING COEFFICIENTS FOR THE SMALL SCALE STRUCTURE

The effects of the small scale structure of the sea will be treated, following an approach pioneered by Rice (Ref. 12), by means of perturbation theory. Only the lowest order corrections to the emissivity of a flat surface will be considered. However, in contrast to the situation exemplified by radar backscattering problems, internal consistency for an emissivity computation requires the inclusion of second order electromagnetic field terms even in the lowest order of computation. Thus, assuming a field

$$\underset{\sim}{E}_{inc} = E_o \hat{A} \, e^{i\underset{\sim}{k}_o \cdot \underset{\sim}{r}} \qquad (\hat{A} = \hat{H}_o \text{ or } \hat{V}_o) \tag{1-22}$$

incident on a homogeneous random surface $z' = f(x', y')$, the scattered field will be written as

$$\underset{\sim}{E}^s_A = R_B^{(o)} E_o \hat{B} \, e^{i\underset{\sim}{k} \cdot \underset{\sim}{r}} + \underset{\sim}{E}^{s(1)}_A + \underset{\sim}{E}^{s(2)}_A \tag{1-23}$$

where $\hat{B} = \hat{H}$ or $\hat{V}$, $R_B^{(0)}$ is the reflection coefficient for a specular surface and $\underset{\sim}{k}$ is the propagation vector in the specular direction relative to $\underset{\sim}{k}_0$. The superscripts 0, 1, and 2 on the right-hand side of (1-23) indicate terms of various orders in powers of the (assumed) small quantities kf, $\frac{\partial f}{\partial x'}$, and $\frac{\partial f}{\partial y'}$. (Note that because the surface with the small scale roughness is assumed to be on an inclined plane, the z' axis coincides locally in direction with the vector n defined in the previous section. For the inclined surface, all geometric quantities are defined as in Figure 1 with the replacement of unprimed quantities by primed quantities.)

Since the scattering coefficients Γ_{AB} are defined in terms of radiation intensities within a small solid angle $d\Omega_s$, the quantities $\langle |\underset{\sim}{E}_A^s \cdot \hat{B}|^2 \rangle$, where the angular brackets indicate expected values, must be expressed as

$$\langle |\underset{\sim}{E}_A^s \cdot \hat{B}|^2 \rangle = \int d\Omega_s \langle |\underset{\sim}{E}_A \cdot \hat{B}|^2 \rangle \qquad (1-24)$$

where $\underset{\sim}{E}_A$ is the electric field in the direction $\hat{k}$. An examination of the derivation given by Peake (Ref. 9) shows that, for purposes of computing Γ_{AB}, the solid angle $d\Omega_s$ must be taken to be

$$d\Omega_s = \frac{A_n \cos\theta'}{R^2} \qquad (1-25)$$

so that

$$\Gamma_{AB} = \frac{4\pi \cos\theta'}{E_0^2 \cos\theta_0'} \langle |\underset{\sim}{E}_A \cdot \hat{B}|^2 \rangle \qquad (1-26a)$$

and

$$\Gamma_B = \frac{4\pi \cos\theta'}{E_0^2 \cos\theta_0'} \langle \text{Re}\left\{ \left(\underset{\sim}{E}_{H_0} \cdot \hat{B} \right) \left(\underset{\sim}{E}_{V_0}^* \cdot \hat{B} \right) \right\} \rangle \qquad (1-26b)$$

10

To exhibit the structure of (1-26) more explicitly, $\underset{\sim}{E}_A$ may be expressed as a sum of various orders in analogy with (1-23):

$$\underset{\sim}{E}_A = R_B^{(o)} E_o \, e^{i \underset{\sim}{k} \cdot \underset{\sim}{r}} \, \hat{B} \, \frac{\delta(\theta' - \theta_o') \, \delta(\varphi' - \varphi_o')}{\sin\theta'} + \underset{\sim}{E}_A^{(1)} + \underset{\sim}{E}_A^{(2)}$$

$$(1-27)$$

If the convention that the expected value $\langle f \rangle$ of the surface height function vanishes is adopted, then $\langle \underset{\sim}{E}_A^{(1)} \rangle$ also vanishes because $\underset{\sim}{E}_A^{(1)}$ is a linear function of f. However, $\langle |\underset{\sim}{E}_A^{(1)}|^2 \rangle$ and $\langle \underset{\sim}{E}_A^{(2)} \rangle$, which are quadratic in f and its derivatives, are not zero. Further information regarding $\langle |\underset{\sim}{E}_A^{(1)}|^2 \rangle$ can be obtained only by solving the appropriate electromagnetic boundary value problem. However, the assumed homogeneous nature of the surface roughness implies translational invariance for the expected value of the electric field strength which, in turn, implies a delta function behavior for $\langle \underset{\sim}{E}_A^{(2)} \rangle$ (this will be demonstrated more explicitly below). Thus, writing

$$\langle \underset{\sim}{E}_A^{(2)} \rangle = E_o \, \underset{\sim}{X}_A \, e^{i \underset{\sim}{k} \cdot \underset{\sim}{r}} \, \frac{\delta(\theta' - \theta_o') \, \delta(\varphi' - \varphi_o')}{\sin\theta'}$$

$$(1-28)$$

it is found, keeping terms up to second order in the surface roughness in (1-26), that

$$\Gamma_{AH} + \Gamma_{AV} = 4\pi\rho_A \, \frac{\delta(\theta' - \theta_o') \, \delta(\varphi' - \varphi_o')}{\sin\theta'} + \frac{4\pi\cos\theta'}{E_o^2 \cos\theta_o'} \left\{ \left\langle |\underset{\sim}{E}_A^{(1)} \cdot \hat{H}|^2 \right\rangle \right.$$

$$\left. + \left\langle |\underset{\sim}{E}_A^{(1)} \cdot \hat{V}|^2 \right\rangle \right\}$$

$$(1-29a)$$

and

$$\Gamma_H + \Gamma_V = \frac{4\pi\cos\theta'}{E_o^2 \cos\theta_o'} \, \text{Re} \left\{ \left\langle \left(\underset{\sim}{E}_{H_o}^{(1)} \cdot \hat{H} \right) \left(\underset{\sim}{E}_{V_o}^{(1)*} \cdot \hat{H} \right) + \left(\underset{\sim}{E}_{H_o}^{(1)} \cdot \hat{V} \right) \left(\underset{\sim}{E}_{V_o}^{(1)*} \cdot \hat{V} \right) \right\rangle \right.$$

$$\left. + E_o^2 \left[R_H^{(o)*} \left(\underset{\sim}{X}_{V_o} \cdot \hat{H} \right) + R_V^{(o)*} \left(\underset{\sim}{X}_{H_o} \cdot \hat{V} \right) \right] \frac{\delta(\theta' - \theta_o') \, \delta(\varphi' - \varphi_o')}{\sin\theta'} \right\}$$

$$(1-29b)$$

where

$$\rho_H = |R_H^{(o)}|^2 + 2 \, \text{Re} \left\{ R_H^{(o)*} \left(\underset{\sim}{X}_{H_o} \cdot \hat{H} \right) \right\} \qquad (1\text{-}30a)$$

$$\rho_V = |R_V^{(o)}|^2 + 2 \, \text{Re} \left\{ R_V^{(o)*} \left(\underset{\sim}{X}_{V_o} \cdot \hat{V} \right) \right\} \qquad (1\text{-}30b)$$

These equations may be substituted into (1-20) and (1-12) to obtain the scattering coefficients of the sea. Of course, the terms containing the delta functions may be integrated analytically to yield rather explicit expressions for the corresponding parts of the scattering coefficients.

To do this, it is convenient to write the delta functions in a form which emphasizes the geometric nature of these terms. Essentially, the delta functions require that the reflected wave propagation vector lie in the plane determined by the incident propagation vector $\hat{k}_o$ and the normal $\hat{n}$ to the reflecting plane. Further, the propagation vector of the reflected wave differs from that of the incident wave only by a change in sign of its component parallel to $\hat{n}$ which implies that $\hat{n}$ is orthogonal to $\hat{k} + \hat{k}_o$. Thus

$$\frac{\delta(\theta' - \theta_o') \, \delta(\varphi' - \varphi_o')}{\sin\theta'} = C \, \delta \left[\hat{n} \cdot (\hat{k}_o + \hat{k}) \right] \delta \left[\hat{n} \cdot \hat{k}_o \times \hat{k} \right] \qquad (1\text{-}31)$$

where C is an invariant to be determined. This is accomplished in the special coordinate system where $\hat{n} = (0, 0, 1)$ where it is found that

$$C = \sin^2\theta_o$$
$$= |\hat{k}_o \times \hat{n}|^2 \qquad (1\text{-}32)$$

Since the second line of (1-32) is expressed in invariant form, it is seen that

$$\frac{\delta(\theta' - \theta_o') \, \delta(\varphi' - \varphi_o')}{\sin\theta'} = |\hat{k}_o \times \hat{n}|^2 \, \delta \left[\hat{n} \cdot (\hat{k}_o + \hat{k}) \right] \delta \left[\hat{n} \cdot \hat{k}_o \times \hat{k} \right] \qquad (1\text{-}33)$$

12

in any coordinate system. With (1-33), the integral in (1-12) may be readily
evaluated by use of standard properties of the delta function. It is found that

$$\delta\left[\hat{n}\cdot(\hat{k}_o + \hat{k})\right]\,\delta\left[\hat{n}\cdot\hat{k}_o\times\hat{k}\right] = \frac{2\,|\hat{k} - \hat{k}_o|^2}{|\hat{k} + \hat{k}_o|^2 B^3}\,\delta\!\left(\zeta_x - \frac{\alpha}{B}\right)\delta\!\left(\zeta_y - \frac{\beta}{B}\right) \qquad (1\text{-}34)$$

where

$$\alpha = (\hat{k} - \hat{k}_o)\cdot\hat{x} = \sin\theta\,\cos\varphi - \sin\theta_o\,\cos\varphi_o \qquad (1\text{-}35a)$$

$$\beta = (\hat{k} - \hat{k}_o)\cdot\hat{y} = \sin\theta\,\sin\varphi - \sin\theta_o\,\sin\varphi_o \qquad (1\text{-}35b)$$

$$B = (\hat{k} - \hat{k}_o)\cdot\hat{z} = \cos\theta + \cos\theta_o \qquad (1\text{-}35c)$$

and $\hat{x}$, $\hat{y}$, and $\hat{z}$ are unit vectors along the x, y, and z coordinate
directions respectively. Further, because of the delta functions, $\hat{n}$ has the
value

$$\hat{n} = (\hat{k} - \hat{k}_o)/\,|\hat{k} - \hat{k}_o| \qquad (1\text{-}36)$$

so that the scalar products $(\hat{h}_o\cdot\hat{H}_o)$ and $(\hat{h}_o\cdot\hat{V}_o)$ in (1-20) may be evaluated
as

$$(\hat{h}_o\cdot\hat{H}) = \hat{h}_o\cdot\hat{k}_o\times\hat{n}/\,|\hat{k}_o\times\hat{n}|$$

$$= \hat{v}_o\cdot\hat{k}/\,|\hat{k}\times\hat{k}_o| \qquad (1\text{-}37a)$$

and

$$(\hat{h}_o\cdot\hat{V}_o) = \hat{h}_o\cdot\hat{H}_o\times\hat{k}_o$$

$$= \hat{h}_o\cdot(\hat{k} - \hat{k}_o\cdot\hat{k}\,\hat{k}_o)/\,|\hat{k}\times\hat{k}_o|$$

$$= \hat{h}_o\cdot\hat{k}/\,|\hat{k}\times\hat{k}_o| \qquad (1\text{-}37b)$$

while the other quantities in (1-12) involving $\hat{n}$ are evaluated as

$$(\hat{n}\cdot\hat{z}) = B/\,|\hat{k} - \hat{k}_o| \qquad (1\text{-}37c)$$

$$(\hat{k}_o\cdot\hat{n}) = \tfrac{1}{2}\,|\hat{k} - \hat{k}_o| \qquad (1\text{-}37d)$$

$$|\hat{k}_o\times\hat{n}|^2 = \tfrac{1}{4}\,|\hat{k}_o + \hat{k}| \qquad (1\text{-}37e)$$

13

Collecting these results, the scattering coefficients of the sea are then given by (taking p in (1-12) to be the two-dimensional Gaussian slope distribution function)

$$\gamma_{hh}(\hat{k}_o, \hat{k}) + \gamma_{hv}(\hat{k}_o, \hat{k}) = \frac{1}{1 + \Lambda(\hat{k}_o) + \Lambda(\hat{k})} \Bigg\{$$

$$\left[\frac{(\hat{v}_o \cdot \hat{k})^2 \rho_h + (\hat{h}_o \cdot \hat{k})^2 \rho_v + 2(\hat{v}_o \cdot \hat{k})(\hat{h}_o \cdot \hat{k}) \rho_{hv}}{(\hat{h}_o \cdot \hat{k})^2 + (\hat{v}_o \cdot \hat{k})^2}\right] \frac{|\hat{k} - \hat{k}_o|^4}{2 \cos\theta_o \, B^4 \, g_{xL} \, g_{yL}}$$

$$\exp\left[-\frac{1}{2B^2}\left(\frac{\alpha^2}{g_{xL}^2} + \frac{\beta^2}{g_{yL}^2}\right)\right] + \frac{1}{(\hat{k}_o \cdot \hat{z})} \int \left[\gamma_{hh}^{(1)}(\hat{n}, \hat{k}_o, \hat{k}) + \gamma_{hv}^{(1)}(\hat{n}, \hat{k}_o, \hat{k})\right]$$

$$\frac{(\hat{k}_o \cdot \hat{n}) \, H(-\hat{k}_o \cdot \hat{n}) \, H(\hat{k} \cdot \hat{n})}{(\hat{n} \cdot \hat{z})} \, p \, d\zeta_x \, d\zeta_y \Bigg\} \tag{1-38a}$$

$$\gamma_{vh}(\hat{k}_o, \hat{k}) + \gamma_{vv}(\hat{k}_o, \hat{k}) = \frac{1}{1 + \Lambda(\hat{k}_o) + \Lambda(\hat{k})} \Bigg\{$$

$$\left[\frac{(\hat{v}_o \cdot \hat{k})^2 \rho_v + (\hat{h}_o \cdot \hat{k})^2 \rho_h - 2(\hat{v}_o \cdot \hat{k})(\hat{h}_o \cdot \hat{k}) \rho_{hv}}{(\hat{h}_o \cdot \hat{k})^2 + (\hat{v}_o \cdot \hat{k})^2}\right] \frac{|\hat{k} - \hat{k}_o|^4}{2 \cos\theta_o \, B^4 \, g_{xL} \, g_{yL}}$$

$$\exp\left[-\frac{1}{2B^2}\left(\frac{\alpha^2}{g_{xL}^2} + \frac{\beta^2}{g_{yL}^2}\right)\right] + \frac{1}{(\hat{k}_o \cdot \hat{z})} \int \left[\gamma_{vh}^{(1)}(\hat{n}, \hat{k}_o, \hat{k}) + \gamma_{vv}^{(1)}(\hat{n}, \hat{k}_o, \hat{k})\right]$$

$$\frac{(\hat{k}_o \cdot \hat{n}) \, H(-\hat{k}_o \cdot \hat{n}) \, H(\hat{k} \cdot \hat{n})}{(\hat{n} \cdot \hat{z})} \, p \, d\zeta_x \, d\zeta_y \Bigg\} \tag{1-38b}$$

where

$$\rho_{hv} = \text{Re}\left\{R_H^{(o)*}\left(\underset{\sim}{X}_{V_o} \cdot \hat{H}\right) + R_V^{(o)*}\left(\underset{\sim}{X}_{H_o} \cdot \hat{v}\right)\right\} \tag{1-39}$$

and $\gamma_{ab}^{(1)}(\hat{n}, \hat{k}_o, \hat{k})$ is that part of $\gamma_{ab}(\hat{n}, \hat{k}_o, \hat{k})$ which contains the contributions of the first order fields $\underset{\sim}{E}_A^{(1)}$.

14

At this point, it is useful to compare these scattering coefficients with results which have been obtained previously by Stogryn (Ref. 1) on the basis of the Kirchhoff approximation. Aside from the factor $\dfrac{1}{1+\Lambda(\hat{k}_o)+\Lambda(\hat{k})}$, which corrects for shadowing effects, the structure of the leading term in both (1-38a) and 1-38b) is similar to that found in Reference 1. In fact, the only differences are: (1) the occurrence of the contributions of the second order terms arising from the small scale roughness in the factors ρ_h, ρ_v and ρ_{hv} and (2) the replacement of the total rms slopes which occurred in the equations in Reference 1 by rms slopes which refer to the large scale structure only. In addition, both (1-38a) and (1-38b) contain integrals over first order electric field terms arising from the small scale structure. These have no counterparts in the equations given in Reference 1. Thus, it is seen that in the limit where the small scale structure vanishes, (1-38a) and (1-38b) reduce to the previous theory with the addition of a correction factor to account for shadowing.

It is now necessary to consider the detailed form of the new terms introduced by the inclusion of the small scale structure. As was indicated earlier, this problem may be solved by means of the small perturbation method of Rice (Ref. 12). It is useful to recall that Rice's method involves a power series expansion of various quantities about the mean height (taken to be $z' = 0$) of the random surface $z' = f(x', y')$ when applying the electromagnetic boundary conditions. In particular, terms of the form $e^{i\underset{\sim}{k}_o \cdot \underset{\sim}{r}}$ and $e^{i\underset{\sim}{k} \cdot \underset{\sim}{r}}$, which describe the incident and scattered waves in the air above the sea, are treated in this manner. This gives rise to the condition

$$k \cos\theta' \sqrt{\langle f^2 \rangle} \quad \ll 1 \qquad\qquad (1-40)$$

In addition, the wave propagating into the sea must be considered in the usual procedure. Since the propagation vector in this case contains an addition factor $\sqrt{K}$ where K is the complex dielectric constant of the water, a further restriction of the form

$$k \left| \sqrt{\langle f^2 \rangle (K - \sin^2\theta')} \right| \ll 1 \qquad\qquad (1-41)$$

arises. This is a much more stringent condition than (1-40) because $|K|>>1$ in the GHz portion of the spectrum (e.g., using the equations given by Stogryn (Ref. 13)*, it is found that for a water salinity of $35^{\circ}/oo$ and a temperature of $20^{\circ}C$, $K = 68.6+65.8i$ at 1.42 GHz, $K = 33.7+36.3i$ at 19.4 GHz, and $K = 16.7+27.1i$ at 37 GHz) and, in fact, would make the small perturbation method of doubtful utility in microwave radiometric studies of the ocean. Fortunately, advantage may be taken of the large size of K by applying Leontovich (impedance) boundary conditions at the air-sea interface rather than requiring the continuity of the tangential components of the electric and magnetic fields at the interface. The Leontovich boundary conditions may be expressed as

$$\underset{\sim}{E} - (\hat{n} \cdot \underset{\sim}{E})\hat{n} = \frac{c}{\sqrt{K}} \, \hat{n} \times \underset{\sim}{B} \qquad (1-42)$$

at the interface where $\underset{\sim}{E}$ and $\underset{\sim}{B}$ are respectively the total electric and magnetic fields at the boundary (in the air) and c is the velocity of light. Since no reference to the fields in the sea itself occurs in (1-42), condition (1-41) is eliminated and the range of validity of the small perturbation method is greatly extended as far as roughness effects are concerned.

However, since (1-42) is not an exact boundary condition for the electromagnetic field, it is useful to check that it does not lead to unacceptable errors arising from its approximate nature. An adequate check is provided by the special case of a perfectly flat surface for which analytical solutions are available for both the exact boundary conditions and (1-42). The exact solutions for the reflection coefficients are the well-known Fresnel coefficients. These are

$$R_h = \frac{\cos\theta_o - \sqrt{K - \sin^2\theta_o}}{\cos\theta_o + \sqrt{K - \sin^2\theta_o}} \qquad (1-43a)$$

---

* There is a typographical error in eq (6) of Reference 13. The coefficient of T should read .40008 instead of 4.0008.

and

$$R_v = \frac{K\cos\theta_o - \sqrt{K-\sin^2\theta_o}}{K\cos\theta_o + \sqrt{K-\sin^2\theta_o}} \qquad (1-43b)$$

for the incident horizontally and vertically polarized waves respectively.
The corresponding results when Maxwell's equations are solved with
boundary conditions (1-42) are

$$R_{hL} = \frac{\cos\theta_o - \sqrt{K}}{\cos\theta_o + \sqrt{K}} \qquad (1-44a)$$

and

$$R_{vL} = \frac{K\cos\theta_o - \sqrt{K}}{K\cos\theta_o + \sqrt{K}} \qquad (1-44b)$$

so that a difference occurs only in terms containing the square roots.
Numerical estimates of the difference between these equations are given in
Table 1 where $|R_a|^2$ and $|R_{aL}|^2$ are shown for some typical cases. Of
course, for a flat surface, the emissivity is simply $1-|R|^2$. It is seen
that the use of (1-42) would lead to calculated brightness temperature errors
less than a small fraction of a degree for a flat sea surface. Since this
error is well below available experimental precision, confidence may be
placed in the application of (1-42) to more complex surfaces bounding the
sea.

With the adoption of boundary conditions (1-42), the computation
of the scattered field proceeds in a manner which closely parallels Rice's
exposition (Ref. 12). Although the algebraic manipulations are lengthy, the
procedure is straightforward and has been sufficiently discussed in the liter-
ature so that the details may be omitted here. The results are:

17

Table 1

COMPARISON OF EXACT AND LEONTOVICH SOLUTION
REFLECTIVITIES FOR A FLAT SEA SURFACE

Water temperature = 20°C, salinity = 35°/oo

ν = 1.42 GHz

θ_0 (degrees)	$|R_h|^2$ (exact)	(Leont.)	$|R_v|^2$ (exact)	(Leont.)
0	0.6830	0.6830	0.6830	0.6830
20	0.6988	0.6990	0.6665	0.6664
40	0.7466	0.7468	0.6078	0.6076
60	0.8263	0.8266	0.4654	0.4648
80	0.9359	0.9360	0.1035	0.1036

ν = 37 GHz

θ_0 (degrees)	$|R_h|^2$ (exact)	(Leont.)	$|R_v|^2$ (exact)	Leont.)
0	0.5386	0.5386	0.5386	0.5386
20	0.5591	0.5591	0.5177	0.5176
40	0.6225	0.6225	0.4459	0.4459
60	0.7339	0.7339	0.2903	0.2907
80	0.8981	0.8982	0.06440	0.0608

Zero Order

The quantity $R_H^{(o)}$ which occurs in (1-30a) and (1-39) is given by (1-44a) while the quantity $R_V^{(o)}$ in (1-30b) and (1-39) is given by (1-44b). In both cases, the angle θ_o is to be replaced by θ_o'. These results are obvious since the zero order computation corresponds to a flat surface.

First Order

The surface height function $z' = f(x', y')$ may be Fourier analyzed as

$$f = \int_{-\infty}^{\infty} dp \int_{-\infty}^{\infty} dq \; P(p, q) \; e^{i(px' + qy')} \qquad (1\text{-}45)$$

where the random function $P(p, q)$ has the properties

$$P(p, q) = P^*(-p, -q) \qquad (1\text{-}46a)$$

$$\langle P(p, q) \rangle = 0 \qquad (1\text{-}46b)$$

$$\langle P(p, q) P^*(p', q') \rangle = \tfrac{1}{4} W(p, q) \delta(p - p') \delta(q - q') \qquad (1\text{-}46c)$$

and W is the roughness spectral density function of the surface normalized so that the mean square height of the small scale structure is given by

$$\langle f^2 \rangle = \tfrac{1}{4} \int_{-\infty}^{\infty} dp \int_{-\infty}^{\infty} dq \; W(p, q) \qquad (1\text{-}47)$$

The first order scattered field is represented as

$$E_A^{s(1)} = \int \underline{e}_A^{(1)} \; P(p - k_o \sin\theta_o' \cos\varphi_o', \; q - k_o \sin\theta_o' \sin\varphi_o')$$

$$e^{i\left[px' + qy' + z'\sqrt{k_o^2 - p^2 - q^2}\right]} dp \, dq \qquad (1\text{-}48)$$

where $e_A^{(1)}$ is a nonrandom function which is determined by the boundary conditions. By use of (1-46c), it is seen that

$$<|\underline{E}_A^{s(1)} \cdot \hat{B}|^2> = \frac{1}{4} \int |\underline{e}_A \cdot \hat{B}|^2 \, W(p - k_o \sin\theta_o' \cos\varphi_o', q - k_o \sin\theta_o' \sin\varphi_o') \, dp \, dq$$

(1-49)

This may be converted to an angular spectrum, as required in (1-24), by use of the transformation

$$p = k_o \sin\theta' \cos\varphi_o' \tag{1-50a}$$

$$q = k_o \sin\theta' \sin\varphi_o' \tag{1-50b}$$

$$dp \, dq = k_o^2 \cos\theta' \, d\Omega_s \tag{1-50c}$$

Thus, the contribution of the first order terms to Γ_{AB} and Γ_B (see (1-26)) may be written as

$$\Gamma_{AB}^{(1)} = 4\pi k_o^4 \cos\theta_o' \cos^2\theta' \, W\left[k_o(\sin\theta' \cos\varphi' - \sin\theta_o' \cos\varphi_o'),\right.$$

$$\left. k_o(\sin\theta' \sin\varphi' - \sin\theta_o' \sin\varphi_o')\right] \alpha_{AB} \tag{1-51a}$$

and

$$\Gamma_B^{(1)} = 4\pi k_o^4 \cos\theta_o' \cos^2\theta' \, W\left[k_o(\sin\theta' \cos\varphi' - \sin\theta_o' \cos\varphi_o'),\right.$$

$$\left. k_o(\sin\theta' \sin\varphi' - \sin\theta_o' \sin\varphi_o')\right] \alpha_B \tag{1-51b}$$

The boundary conditions (1-42), when used in conjunction with the representation for the first order field determine the functions α_{AB} and α_B. These are

$$\alpha_{HH} = \left|\frac{(K-1)\cos(\varphi' - \varphi_o') + \sin\theta' \sin\theta_o'}{(\sqrt{K'} + \cos\theta_o')(\sqrt{K} + \cos\theta')}\right|^2 \tag{1-52a}$$

20

$$\alpha_{HV} = \left| \frac{(K - 1)\sin(\varphi' - \varphi_0')}{\left(\sqrt{K} + \cos\theta_0'\right)\left(\sqrt{K}\cos\theta' + 1\right)} \right|^2 \tag{1-52b}$$

$$\alpha_{VH} = \left| \frac{(K - 1)\sin(\varphi' - \varphi_0')}{\left(\sqrt{K} + \cos\theta'\right)\left(\sqrt{K}\cos\theta_0' + 1\right)} \right|^2 \tag{1-52c}$$

$$\alpha_{VV} = \left| \frac{K\sin\theta'\sin\theta_0' - (K - 1)\cos(\varphi - \varphi_0')}{\left(\sqrt{K'}\cos\theta_0' + 1\right)\left(\sqrt{K}\cos\theta' + 1\right)} \right|^2 \tag{1-52d}$$

$$\alpha_H = \mathrm{Re}\left\{ \frac{(K - 1)\cos(\varphi' - \varphi_0') + \sin\theta'\sin\theta_0'}{\left(\sqrt{K} + \cos\theta_0'\right)\left(\sqrt{K} + \cos\theta'\right)} \cdot \right.$$
$$\left. \left(\frac{(K - 1)\sin(\varphi' - \varphi_0')}{\left(\sqrt{K} + \cos\theta'\right)\left(\sqrt{K}\cos\theta_0' + 1\right)} \right)^* \right\} \tag{1-52e}$$

$$\alpha_V = \mathrm{Re}\left\{ \frac{(K - 1)\sin(\varphi' - \varphi_0')}{\left(\sqrt{K} + \cos\theta_0'\right)\left(\sqrt{K}\cos\theta' + 1\right)} \cdot \right.$$
$$\left. \left(\frac{K\sin\theta'\sin\theta_0' - (K - 1)\cos(\varphi' - \varphi_0')}{\left(\sqrt{K}\cos\theta_0' + 1\right)\left(\sqrt{K}\cos\theta' + 1\right)} \right)^* \right\} \tag{1-52f}$$

It is interesting to note that the expressions for α_{AB} and α_B reduce to the standard, known results for perfect conductors in the limit as $K \to \infty$. However, for a large, but finite dielectric constant, these coefficients imply a slightly different angular dependence for the scattered field than that which would have resulted from the solution of the boundary value problem in which the tangential components of the electric and magnetic fields are required to be continuous across the boundary.

Second Order

The second order field is obtained from the substitution of (1-23) (and the corresponding experssion for the magnetic field) into (1-42) and using the results discussed above for the zero and first order fields. It is clear from the nature of the method that $E_A^{s(2)}$ will depend quadratically on the height function both explicitly through terms containing f^2 and various combinations of derivatives and through products of f, $\frac{\partial f}{\partial x'}$, and $\frac{\partial f}{\partial y'}$ with $E_A^{s(1)}$. Upon computing expected values, terms explicitly quadratic in f and its derivatives will yield terms proportional to the mean square height and slope of the surface times a plane wave propagation factor. These, obviously lead to delta function parts for $\langle E_A^{(2)} \rangle$ when $\langle E_A^{s(2)} \rangle$ is decomposed into an angular spectrum of waves. Likewise, products with $E_A^{s(1)}$ will lead to delta functions. As a typical case, consider $\langle f\, E_A^{s(1)} \rangle$. Using (1-45) through (1-48) together with the standard theorem that the Fourier transform of a product of functions is the convolution of Fourier transforms, it is found that

$$\langle f\, E_A^{s(1)} \rangle = \int dp\, dq\; e^{i\left[px' + qy' + z'\sqrt{k_o^2 - p^2 - q^2}\right]} \delta(p - k_o \sin\theta_o' \cos\varphi_o')$$

$$\delta(q - k_o \sin\theta_o' \sin\varphi_o') \cdot \frac{1}{4}\int dp'\, dq'\, e_A^{(1)}\, w(p'-p, q'-q)$$

$$(1-53)$$

Hence, using (1-50), it is seen that terms of this type also lead to delta function terms in the angular spectrum. Thus, the form of (1-28) is verified.

Explicit expressions for X_A, of course, are obtained only through a considerable amount of algebraic computation. The results may be expressed as

$$X_A = \frac{\sqrt{K}}{\sqrt{K} + \cos\theta_o'}\, S_A\, \hat{H} - \frac{\sqrt{K}}{\sqrt{K}\cos\theta_o' + 1}\, P_A\, \hat{V} \qquad (1-54)$$

where

$$S_{H_o} = \frac{\cos\theta_o'}{\sqrt{K} + \cos\theta_o'} \Bigg((g_{xs}^2 - g_{ys}^2)(\sin^2\varphi_o' - \cos^2\varphi_o') + \frac{1}{2\sqrt{K}} \int dp\, dq\, W \Big\{$$

$$\Big[k_o(K-1) + \sin\theta_o'(q\sin\varphi_o' + p\cos\varphi_o') \Big] \sqrt{k_o^2 - p^2 - q^2}$$

$$+ \frac{\sqrt{K}(K-1)\,k_o\,(q\cos\varphi_o' - p\sin\varphi_o')^2}{\sqrt{K}\sqrt{k_o^2 - p^2 - q^2} + k_o}$$

$$- \frac{\Big[k_o\sin\theta_o' - (p\cos\varphi_o' + q\sin\varphi_o')\Big]\Big[k_o(K-1)(p\cos\varphi_o' + q\sin\varphi_o') + \sin\theta_o'(p^2 + q^2)\Big]}{k_o\sqrt{K} + \sqrt{k_o^2 - p^2 - q^2}} \Big\} \Bigg)$$

$$(1\text{-}55a)$$

$$P_{H_o} = \frac{\cos\theta_o'}{\sqrt{K} + \cos\theta_o'} \Bigg(2(g_{xs}^2 - g_{ys}^2)\sin\varphi_o'\cos\varphi_o' + \frac{1}{2\sqrt{K}} \int dp\, dq\, W \Big\{$$

$$- \sin\theta_o'\,(p\sin\varphi_o' - q\cos\varphi_o')\sqrt{k_o^2 - p^2 - q^2}$$

$$+ \frac{\sqrt{K}(K-1)\Big[q\cos\varphi_o' - p\sin\varphi_o'\Big]\Big[k_o\sin\theta_o' - p\cos\varphi_o' - q\sin\varphi_o'\Big]}{\sqrt{K}\sqrt{k_o^2 - p^2 - q^2} + k_o}$$

$$- \frac{\Big[p\sin\varphi_o' - q\cos\varphi_o'\Big]\Big[k_o(K-1)(p\cos\varphi_o' + q\sin\varphi_o') + \sin\theta_o'(p^2 + q^2)\Big]}{k_o\sqrt{K} + \sqrt{k_o^2 - p^2 - q^2}} \Big\} \Bigg)$$

$$(1\text{-}55b)$$

23

$$S_{V_o} = \frac{\cos\theta_o'}{\sqrt{K}\cos\theta_o' + 1}\left(2(g_{xs}^2 - g_{ys}^2)\sin\varphi_o'\cos\varphi_o' + \frac{1}{2\sqrt{K}}\int dp\, dq\, W\left\{\vphantom{\int}\right.\right.$$

$$- K\sin\theta_o'(p\sin\varphi_o' - q\cos\varphi_o')\sqrt{k_o^2 - p^2 - q^2}$$

$$- \frac{\sqrt{K}\left[q\cos\varphi_o' - p\sin\varphi_o'\right]\left[k_o(K-1)(p\cos\varphi_o' + q\sin\varphi_o') - K\sin\theta_o'(p^2 + q^2)\right]}{\sqrt{K}\sqrt{k_o^2 - p^2 - q^2} + k_o}$$

$$\left.\left. + \frac{k_o(K-1)\left[p\sin\varphi_o' - q\cos\varphi_o'\right]\left[k_o\sin\theta_o' - p\cos\varphi_o' - q\sin\varphi_o'\right]}{k_o\sqrt{K} + \sqrt{k_o^2 - p^2 - q^2}}\right\}\right)$$

<div align="right">(1-55c)</div>

$$P_{V_o} = \frac{\cos\theta_o'}{\sqrt{K}\cos\theta_o' + 1}\left((g_{xs}^2 - g_{ys}^2)(\cos^2\varphi_o - \sin^2\varphi_o) + \frac{1}{2\sqrt{K}}\int dp\, dq\, W\left\{\vphantom{\int}\right.\right.$$

$$\left[k_o(K-1) - K\sin\theta_o'(p\cos\varphi_o' + q\sin\varphi_o')\right]\sqrt{k_o^2 - p^2 - q^2}$$

$$- \frac{\sqrt{K}\left[k_o\sin\theta_o' - p\cos\varphi_o' - q\sin\varphi_o'\right]\left[k_o(K-1)(p\cos\varphi_o' + q\sin\varphi_o') - K\sin\theta_o'(p^2 + q^2)\right]}{\sqrt{K}\sqrt{k_o^2 - p^2 - q^2} + k_o}$$

$$\left.\left. + \frac{k_o(K-1)(p\sin\varphi_o' - q\cos\varphi_o')^2}{k_o\sqrt{K} + \sqrt{k_o^2 - p^2 - q^2}}\right\}\right)$$

<div align="right">(1-55d)</div>

where g_{xs}^2 and g_{yx}^2 are the mean square slopes of the small scale structure in the x$'$ and y$'$ directions respectively. The first and second arguments of W in (1-55) are $p - k_o\sin\theta_o'\cos\varphi_o'$ and $q - k_o\sin\theta_o'\sin\varphi_o'$ respectively.

These equations complete the specification of the quantities required for the solution of the electromagnetic boundary value problem.

1.4 DESCRIPTION OF THE SEA SURFACE

In the preceding section, equations were developed for the scattering coefficients of the sea. The expressions which were obtained depend on the rms slopes g_{xL} and g_{yL} of the large scale wave structure and the rms slopes g_{xs} and g_{ys} of the small scale structure in two orthogonal directions. The roughness spectral density function $W(K_x, K_y)$ for the small scale wave structure is also required. The specification of these quantities will be considered here. The orientation of the coordinate system will be chosen so that the x coordinate is in the cross wind direction while the y coordinate is in the up wind direction.

One of the basic experiments relating to the description of the sea surface was performed by Cox and Munk (Refs. 14 and 15) who demonstrated that the slope distribution function of the sea was nearly Gaussian with mean square slopes

$$g_x^2 = 0.003 + 1.92 \times 10^{-3} \, w \pm 0.002 \qquad (1\text{-}56a)$$

$$g_y^2 = 3.16 \times 10^{-3} \, w \pm 0.004 \qquad (1\text{-}56b)$$

in the cross wind and up wind directions respectively. Here w is the wind speed, in m/sec, at a height of 41 feet above the sea surface. Of course, the actual values of the ratio $(g_y/g_x)^2$ will vary considerably due to fluctuations in the wind direction and Cox and Munk found values ranging from 1.0 to 1.8. Values of this ratio close to 1 are expected for gusty winds while steady winds lead to higher values.

For the two-scale scattering model, it is necessary to consider the slopes given by (1-56) to arise from the addition of independent random surfaces representing the large and small scale roughness so that

$$g_x^2 = g_{xL}^2 + g_{xs}^2 \qquad (1\text{-}57a)$$

$$g_y^2 = g_{yL}^2 + g_{yx}^2 \qquad (1\text{-}57b)$$

25

To obtain explicit expressions for the decomposition (1-57), it is necessary to consider the spectral function $W(K_x, K_y)$ of the sea surface. This function will be normalized so that if the height of the sea above its mean level is given by the random function $z = \zeta(x, y)$ then the mean square height is given by

$$<\zeta^2> = \frac{1}{4} \int_{-\infty}^{\infty} dK_x \int_{-\infty}^{\infty} dK_y \, W(K_x, K_y) \qquad (1-58)$$

It is also convenient to use the alternate representation in polar coordinates

$$<\zeta^2> = \int_{0}^{\infty} W(k) \, K dK \qquad (1-59)$$

where

$$W(K) = \frac{1}{4} \int_{0}^{2\pi} W(K \cos\beta, \, K \sin\beta) \, d\beta \qquad (1-60)$$

Here, $K_x = K \cos\beta$ and $K_y = K \sin\beta$. In terms of the polar representation,

$$\frac{1}{4} W(K_x, K_y) = W(K) \, G(\beta) \qquad (1-61)$$

where

$$\int_{0}^{2\pi} G(\beta) \, d\beta = 1 \qquad (1-62)$$

Expressions for the directional function $G(\beta)$ will be considered later.

The small scale wave structure of the sea is determined by the high wave number components of the function $W(K)$. Those components for which K is greater than some value, K_{min}, will contribute an amount

$$<\zeta^2>_s = \int_{K_{min}}^{\infty} W(K) \, K dK \qquad (1-63)$$

to the mean square height of the sea and this may be identified with the mean square height $\langle f^2 \rangle$ of the small scale structure considered in the previous section. Since the small perturbation method requires that $k^2 \langle \zeta^2 \rangle_s$ be small, the wave number K_{min} may be determined by the condition

$$k\sqrt{\langle \zeta^2 \rangle_s} = a \tag{1-64}$$

where a is a sufficiently small number (say, 0.1 to 0.4). Thus, for example, if W is given by the Phillips form

$$W(K) = \frac{A}{K^4} \tag{1-65}$$

(for K not too small) where A is a dimensionless constant with a value of about 5.85×10^{-3}, it is found that

$$K_{min} = \sqrt{\frac{A}{2}} \frac{k}{a} \tag{1-66}$$

$$\approx 5.41 \times 10^{-2} \frac{k}{a}$$

Hence, the largest wavelength of the sea which will be assigned to the small scale structure will range from about 2 to 8 electromagnetic wavelengths if a is chosen in the range 0.1 to 0.4. The precise choice of a does not appear to be too critical, especially for a near 0.4, since the geometric optics method should be applicable to sea waves whose length is several electromagnetic wavelengths. Hence these waves may, with equal validity, be assigned to either the large or the small scale structure of the sea.

With a choice of K_{min} as discussed above, it is now possible to specify the mean square slopes of the large and small scale structure. This may be accomplished by determining g_{xL}^2 and g_{yL}^2 and then using (1-56) in conjunction with (1-57) to find g_{xs}^2 and g_{ys}^2. Thus,

$$g_{xL}^2 = \int K^2 \cos^2\beta \; W \; Kd \; Kd\beta$$

$$g_{xL}^2 = \int_{K<K_{min}} W(K) \; K^3 dK \int_0^{2\pi} \cos^2\beta \; G(\beta) \; d\beta \qquad (1\text{-}67a)$$

$$g_{yL}^2 = \int_{K<K_{min}} W(K) \; K^3 \; dK \int_0^{2\pi} \sin^2\beta \; G(\beta) \; d\beta \qquad (1\text{-}67b)$$

If the Phillips spectrum (1-65) is chosen to represent the sea surface, the integrals over K in (1-67) may be readily performed (it should be noted that there is a sharp, wind dependent, lower cut-off to the spectrum given by (1-65) at a wave number equal to g/w^2 where g is the acceleration due to gravity). It is found that

$$g_{xL}^2 = A \; \ell n \left(\frac{K_{min}}{g/w^2} \right) \int_0^{2\pi} \cos^2\beta \; G(\beta) \; d\beta \qquad (1\text{-}68a)$$

$$g_{yL}^2 = A \; \ell n \left(\frac{K_{min}}{g/w^2} \right) \int_0^{2\pi} \sin^2\beta \; G(\beta) \; d\beta \qquad (1\text{-}68b)$$

Thus, if $G(\beta)$ were specified, all of the required slopes can be found.

Current information is not sufficient to determine the complete form of $G(\beta)$ without the introduction of special hypotheses. $G(\beta)$ is expected to be large in the up wind direction and become zero in the range $\pi < \beta < 2\pi$. A specific form suggested by Pierson (Ref. 16) is

$$G(\beta) = \begin{cases} \dfrac{1}{\pi}\left[\dfrac{1}{2} + \sin^2\beta\right] & 0 \le \beta \le \pi \\[4mm] 0 & \pi < \beta < 2\pi \end{cases} \qquad (1\text{-}69)$$

This leads to the ratio $(g_x/g_y)^2 = \frac{3}{5}$ (independent of the functional form of W(K)) and is very close to the value 0.608 which is obtained from (1-56) in the limit of large wind speeds. For lower wind speeds, there is some discrepancy between (1-69) and (1-56) and, for internal consistency, it is desirable to modify (1-69). The form

28

$$G(\beta) = \begin{cases} \dfrac{1}{\pi}\left[c_1(w) + c_2(w)\sin^2\beta\right] & 0 \le \beta \le \pi \\[2mm] 0 & \pi < \beta < 2\pi \end{cases} \qquad (1\text{-}70)$$

is suggested here where c_1 and c_2 are wind dependent coefficients. The normalization (1-62) implies that

$$c_1(w) = 1 - \frac{1}{2}c_2(w) \qquad (1\text{-}71)$$

while the fact that

$$\frac{g_x^2}{g_y^2} = \frac{\int \cos^2\beta \, G \, d\beta}{\int \sin^2\beta \, G \, d\beta} = \frac{\frac{1}{2}\left[1 - \frac{1}{4}c_2\right]}{\frac{1}{2}\left[1 + \frac{1}{4}c_2\right]} \qquad (1\text{-}72)$$

shows, in conjunction with (1-56), that

$$c_2(w) = 4\,\frac{g_y^2 - g_x^2}{g_y^2 + g_x^2}$$

$$= 4\,\frac{1.24 \times 10^{-3}w - 3 \times 10^{-3}}{3 \times 10^{-3} + 5.08 \times 10^{-3}w} \qquad (1\text{-}73)$$

REFERENCES

(1) A. Stogryn, "The apparent temperature of the sea at microwave frequencies," IEEE Trans. on Antennas and Propagation, vol AP-15, 1967, pp 278-286.

(2) J. Hollinger, "Passive microwave measurements of the sea surface," J. Geophys. Res., vol 75, 1970, pp 5209-5213.

(3) J. Hollinger, "Passive microwave measurements of sea surface roughness," IEEE Trans. Geoscience Electronics, vol GE-9, 1971, pp 165-169.

(4) W. Nordberg, J. Conaway, and P. Thaddeus, "Microwave observations of sea state from aircraft," Q. J. Royal Met. Soc., vol 95, 1969, pp 408-413.

(5) W. Nordberg, J. Conaway, D. Ross, and T. Wilheit, "Measurements of microwave emission from a foam covered, wind driven sea," J. Atmos. Sciences, vol 28, 1971, pp 429-435.

(6) G. Williams, "Microwave radiometry of the ocean and the possibility of marine wind velocity determination from satellite observations," J. Geophys. Res., vol 74, 1969, pp 4591-4594.

(7) G. Williams, "Microwave emissivity measurements of bubbles and foam," IEEE Trans. Geoscience Electronics, vol GE-9, 1971, pp 221-224.

(8) A. Stogryn, "The emissivity of sea foam at microwave frequencies," Aerojet report prepared under Contract NAS 1-10633, April 1970. (Accepted for publication in J. Geophys. Res. Also, see Appendix A of this report.)

(9) W. Peake, "Interaction of electromagnetic waves with some natural surfaces," IRE Trans. on Antennas and Propagation, vol AP-7, pp S324-S329.

(10) M. Sancer, "Shadow corrected electromagnetic scattering from a randomly rough surface," IEEE Trans. on Antennas and Propagation, vol AP-17, 1969, pp 577-585.

(11) B. Smith, "Geometrical shadowing of a random rough surface," IEEE Trans. on Antennas and Propagation, vol AP-15, 1967, pp 668-671.

(12) S. Rice, "Reflection of electromagnetic waves from slightly rough surfaces," Comm. Pure and Appl. Math., vol 4, 1951, pp 351-378.

(13) A. Stogryn, "Equations for calculating the dielectric constant of saline water," IEEE Trans. on Microwave Theory and Techniques, vol MTT-19, 1971, pp 733-736.

(14)   C. Cox and W. Munk, "Measurements of the roughness of the sea surface from photographs of the sun's glitter," J. Opt. Soc. Am., vol 44, 1954, pp 838-850.

(15)   C. Cox and W. Munk, "Statistics of the sea surface derived from sun glitter," J. Marine Res., vol 13, 1954, pp 198-227.

(16)   W. Pierson, "A proposed vector wave number spectrum for the study of radar sea return," in Microwave Observation of the Ocean Surface, U. S. Naval Oceanographic Office, SP-152 (1969).

Section 2

THE BRIGHTNESS TEMPERATURE OF THE SEA

2.1 INTRODUCTION

Because of its potential use as a means of studying oceanographic and meteorological phenomena, the microwave radiometric characteristics of the sea have recently received a considerable amount of study. The first published theoretical study relating to the brightness temperature of the ocean (Ref. 1) considered only the effects of the large scale wave structure in the Kirchhoff approximation and resulted in predictions that subsequently received partial verification by some experiments (Refs. 2 and 3). However, other experiments under different conditions (Refs. 4, 5 and 6) have yielded results at variance with the original theory and have led to an interpretation of the brightness temperature data in terms of the emission properties of sea foam to the exclusion of waves. A considerable amount of confusion has thus developed regarding the physical basis for the observed brightness temperature characteristics of the sea.

A thorough examination of the theoretical and experimental evidence shows that an interpretation in terms of only foam or only waves cannot yield an adequate explanation of all of the observed phenomena. While a limited portion of the available data may be explained by invoking only one of these mechanisms, a comprehensive picture of the microwave properties of the sea must include the effects of both waves and foam. It is shown, in this report, how all of the essential features regarding the brightness temperature changes of the sea may be explained by an appropriate combination of these effects. There are, of course, still some details — both theoretical and experimental— which need to be examined more closely in order to achieve a complete grasp of the microwave characteristics of the ocean.

2.2   BASIC EQUATIONS

The brightness temperature of the radiation with polarization p emanating from the surface of the sea at angle θ with respect to the vertical, and angle φ with respect to the local wind direction may be expressed as

$$T_p(\nu,\theta,\varphi) = f\,T_{pF}(\nu,\theta) + (1-f)\,T_{pW}(\nu,\theta,\varphi) \qquad (2-1)$$

where f is the fraction of the sea surface covered with foam, T_{pF} is the brightness temperature of the foam and T_{pW} the brightness temperature of the foam-free water. This radiation will, in propagating through the atmosphere, undergo some modification as is discussed in Reference 1. However, atmospheric effects will not be considered in detail here. Rather, attention will be confined to the individual terms exhibited in (2-1).

The term $T_{pF}(\nu,\theta)$ has been considered in detail in Reference 7. According to Reference 7

$$T_p(\nu,\theta) = \epsilon_p(\nu,\theta)\,T_W + \left[1 - \epsilon_p(\nu,\theta)\right] T_{sky}(\nu,\theta) \qquad (2-2)$$

where T_W is the water thermal temperature, T_{sky} the incident sky brightness temperature and ϵ_p the emissivity of the foam. Explicit equations, based on experimental measurements are given for ϵ_p in Reference 7 and will not be repeated here. T_{sky}, of course, depends on prevailing atmospheric conditions and does not depend on the state of the sea.

The second term, T_{pW}, in (2-1) depends upon the bistatic scattering coefficients of the sea as well as on the incident sky temperature. Because the wave structure of the sea is not isotropic, a dependence on the wind direction is also introduced. Precise equations in terms of the scattering coefficients are given in Reference 1. Calculations based upon the Kirchhoff approximation for the scattering coefficients were also discussed in Reference 1. However, an extension of the basic theory is now available (Ref. 8) so that somewhat refined calculations may be made. The principal

new feature with regard to wave effects in the calculations to be discussed below is the inclusion of shadowing corrections as is discussed in Reference 8 as well as the use of more precise results for the dielectric properties of sea water (Ref. 9)*. It is found that shadowing corrections are negligible for small angles θ, but gradually become more significant at angles greater than 60° and for high sea states. While the theory discussed in Reference 8 also shows how the influence of the small scale wave structure of the sea may be accounted for without the use of the Kirchhoff approximation, the small scale effects have not, as yet, been included in the numerical calculations.

The final factor occurring in (2-1) which must be considered is the fractional foam coverage f. While the growing literature on the subject (Refs. 10 through 14) shows that increasing attention is being given to the measurement of the foam coverage of the sea, it is evident that much remains to be accomplished — especially in the range of very high wind speeds.

The available results on foam coverage are generally analyzed in terms of wind speed. When this is done, a large scatter in the data is immediately evident and must be ascribed to the incomplete description which considers the local wind speed alone. Other factors which are known to affect the foam cover and which ultimately must be considered include the fetch and duration of the wind, water temperature, thermal stability (i.e., whether the air temperature is higher or lower than the water temperature), water salinity, and variations in the surface tension of the water due to the occurrence of organic films. Since, at the present time, it is premature to attempt an analysis of foam coverage based on all of these factors, the present discussion will be confined principally to the wind speed dependence.

Figure 2 shows the percentage foam cover as a function of wind speed using data from a variety of sources. These include Murphy's re-analysis of Blanchard's (Ref. 10) original data as well as aircraft data discussed in Reference 11. The data of Monahan (Ref. 13) on ocean whitecaps

---

* Note the following typographical error in Reference 9. The coefficient of T equation (6) of (9) should read 0.40008 instead of 4.0008.
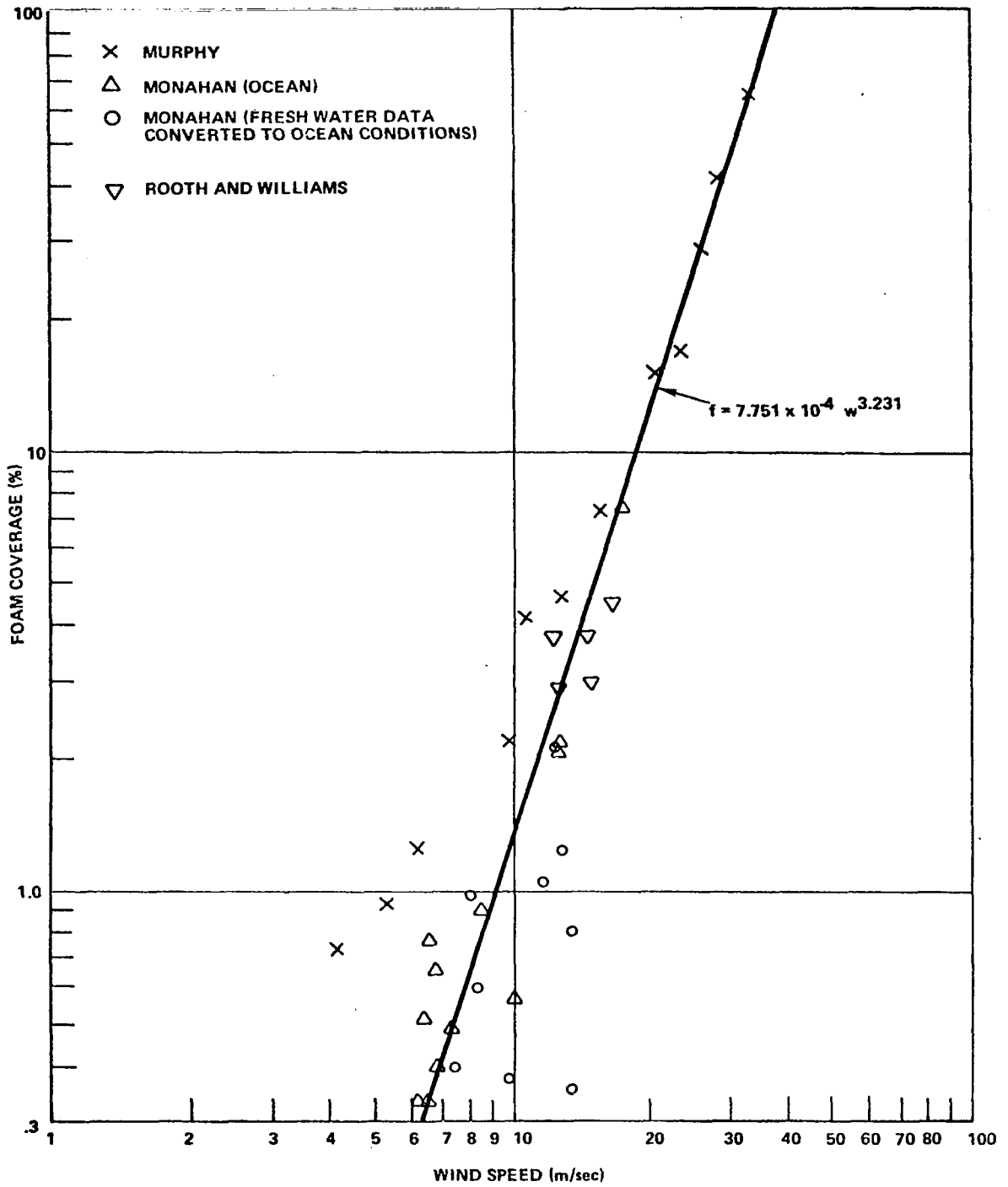
Figure 2.   Foam Coverage as a Function of Wind Speed Over
The Sea

35

as well as fresh water whitecaps (Ref. 12) (which, as suggested in Reference 13, can be converted to oceanic conditions by multiplying the foam cover by 1.51) were obtained from an analysis of shipboard data. In order to avoid excessive cluttering of the figure, only some representative points, indicating the data trends and uncertainties, have been plotted from References 12 and 13 at the lower wind speeds. In the higher wind speed range, which is of greatest interest from the point of view of microwave radiometry, all of the known data are plotted.

The large scatter of the data in Figure 2 is evident. While the scatter appears to decrease at higher wind speeds, this may be an illusory effect since much less data is available in this region. Nevertheless, a curve fit, which heavily weighted the high wind speed range, was made with the result that the foam cover is given as

$$f = 7.751 \times 10^{-4} \ w^{3.231} \tag{2-3}$$

percent where w is the wind speed in m/sec. Since f reaches a value of 100 percent for $w \approx 38$ m/sec, (2-3) must, of course, not be used above such a wind speed. This equation was used in the computations to be discussed below.

2.3 SOME NUMERICAL RESULTS

Some numerical calculations made on the basis of the equations described in the previous section will be discussed here. These results may be compared with the published measurements of Hollinger (Refs. 2 and 3) for a sea in which observations of foam patches have been excluded and with Nordberg, et al (Ref. 5) for sea conditions which included both waves and foam.

Hollinger (Refs. 2 and 3) has already presented a comparison of his results with the version of the theory given by Stogryn (Ref. 1). In verification of the theory, he found that the vertically polarized brightness temperature was quite insensitive to the wind speed at an angle near 55° at each of his measurement frequencies (1.41, 8.36 and 19.34 GHz). Also qualitative agreement was found with the theoretical predictions for horizontal polarization. The agreement was best at 19.34 GHz but progressively grew worse

at the lower frequencies, the principal discrepancy being that the theory predicted too large a wind speed dependence for the brightness temperature. Since the principal new feature with regard to wave effects which was introduced in the present computations was the inclusion of a shadowing correction, and this is frequency independent and is prominent only at large angles, the new computation did not alter the state of affairs. However, it is conjectured that had the complete theory in Reference 8 been programmed, the agreement with Hollinger's data would have materially improved since, at low frequencies, a progressively larger part of the wave structure would have been included in the small scale structure and hence resulted in more isotropic scattering.

Since the data of Hollinger did indicate a fair agreement between the predictions of the theory and experiment at 19.4 GHz and horizontal polarization, a comparison with the data of Nordberg, et al (Ref. 5) is quite enlightening. In this case, both waves and foam were present on the sea surface. However, because only horizontally polarized brightness temperatures were measured, further comparisons with experiment cannot be made for vertical polarization. Two interesting cases are shown in Reference 5 (see Figure 3 of the reference). One (labeled Case F) refers to a situation in which the wind speed was 25 m/sec while the other (labeled Case B) refers to a wind speed of 6 m/sec. The authors of Reference 5 believe that an absolute calibration error of 10 to 15°K exists in their data. On the basis of their estimates for a smooth sea surface and Case B at nadir, an error of 15°K will be assumed here. The atmospheric conditions described in Reference 5 imply a sky brightness temperature of approximately 19°K at zenith and a model atmosphere which yielded a sky brightness temperature of 18.9°K at zenith was used in the computations to be discussed here. There are no other adjustable factors in the theory so that a rather stringent test is available.

Figure 3 compares the results of Reference 5, adjusted for the calibration error, with the present theory (which includes shadowing, foam, and the large scale wave structure without a separate treatment of small scale effects). Also shown, for reference purposes, is the brightness temperature of a specular sea surface (this differs at large angles from the smooth
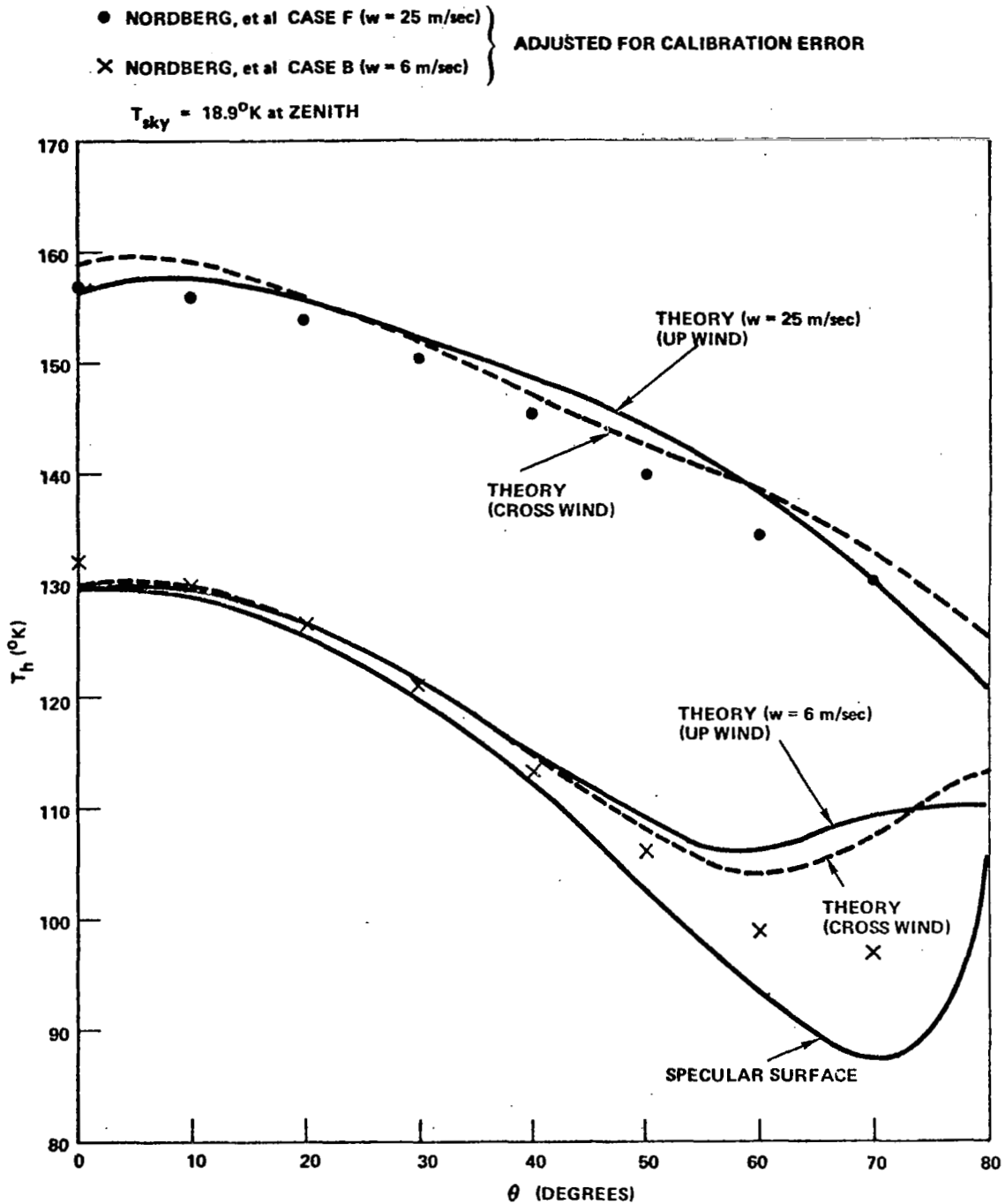
Figure 3. Horizontally Polarized Brightness Temperature as a
Function of Angle at 19.4 GHz

sea curve computed in the reference. The latter does not appear to be correct to the present author). It is seen that the theory agrees quite closely with the experimental data at a wind speed of 6 m/sec from nadir to an angle of about 40° at which point the deviation becomes noticeable. This trend is in agreement with Hollinger's results which indicated a smaller wind speed dependence for the experimental data than predicted by the theory. In fact, further computation (not shown in Figure 3) indicates close agreement between theory and experiment to angles above 60° if the rms slope of the waves is multiplied by a factor of about 5/6 (corresponding to a wind speed of 4 m/sec). The experimental data at a wind speed of 25 m/sec also shows a slight tendency to fall below the theory. The source of this discrepancy appears to be the same as above. It is interesting to notice the wide separation between the curves at wind speeds of 6 and 25 m/sec. At small angles, this is the direct result of the inclusion of foam in the calculation and is distinctly different than results which would have been obtained by considering wave geometry effects alone.

In view of the above comparisons with available experimental data, one may expect that the predictions of the current theory under other conditions will be reasonably accurate at 19.4 GHz, better at higher frequencies, and somewhat poorer at lower frequencies. With this admonition in mind, computations of both the horizontally and vertically polarized brightness temperatures at frequencies of 19.4, 37, and 13.4 GHz are shown in Figures 4, 5, and 6 respectively. In all cases, the assumed atmospheric conditions correspond to that used in the discussion of the data of Reference 5 above. A water thermal temperature of 290°K and a water salinity of $35^\circ/$oo is assumed. The temperatures shown in the figures correspond to those which would be observed from a low flying aircraft with the radiometers pointing in the cross-wind direction. It is to be noted that at wind speeds less than 10 m/sec, the results do not differ greatly from those which would have been obtained had foam been neglected entirely and qualitatively are similar to curves published previously in Reference 1. At higher wind speeds, qualitative changes in shape for both the cases of horizontal and vertical polarization occur together with quantitative differences. This is due primarily to the foam although at large angles the inclusion of shadowing in the calculations
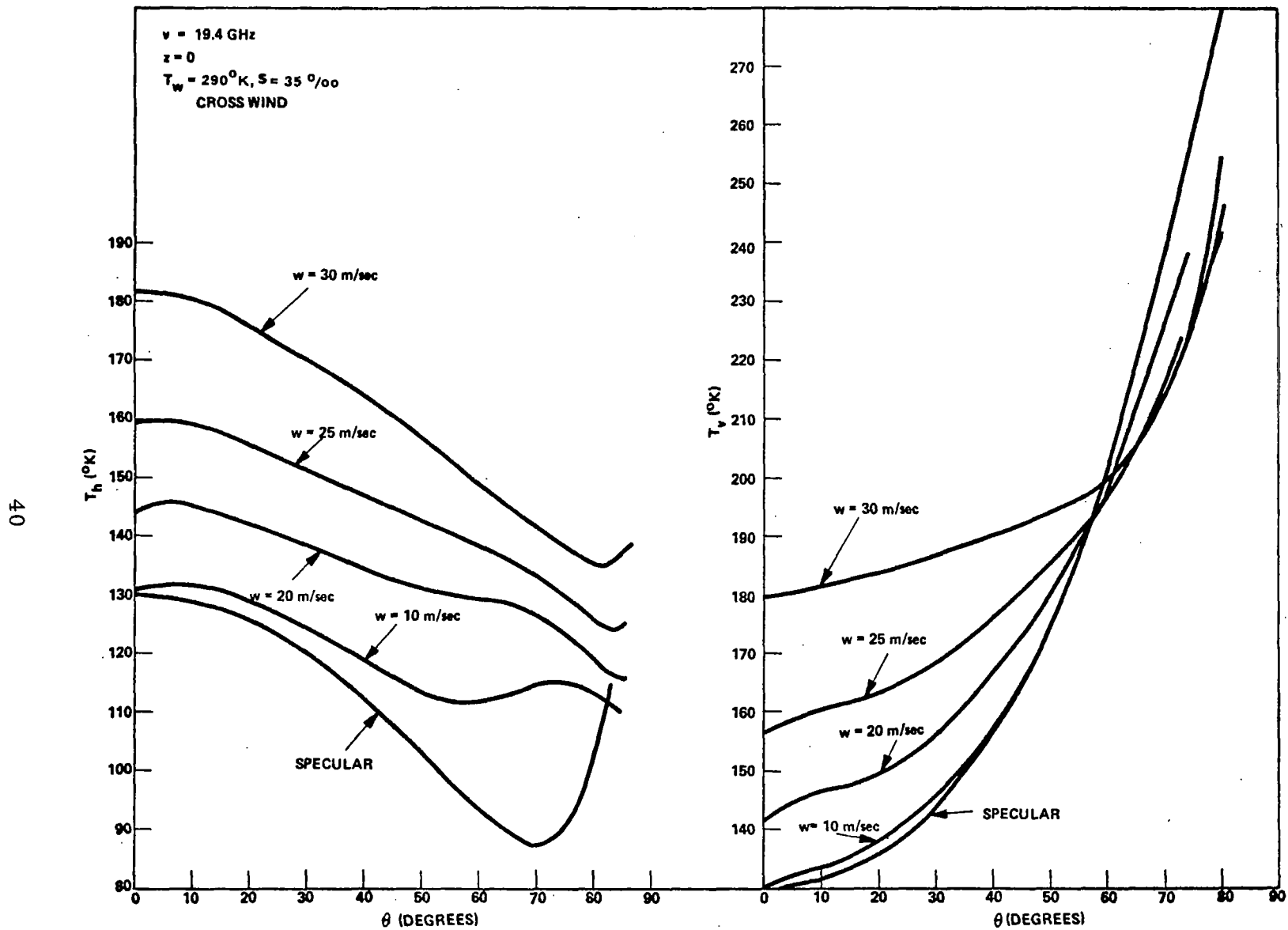
Figure 4. Horizontally and Vertically Polarized Brightness Temperatures at 19.4 GHz for Various Wind Speeds
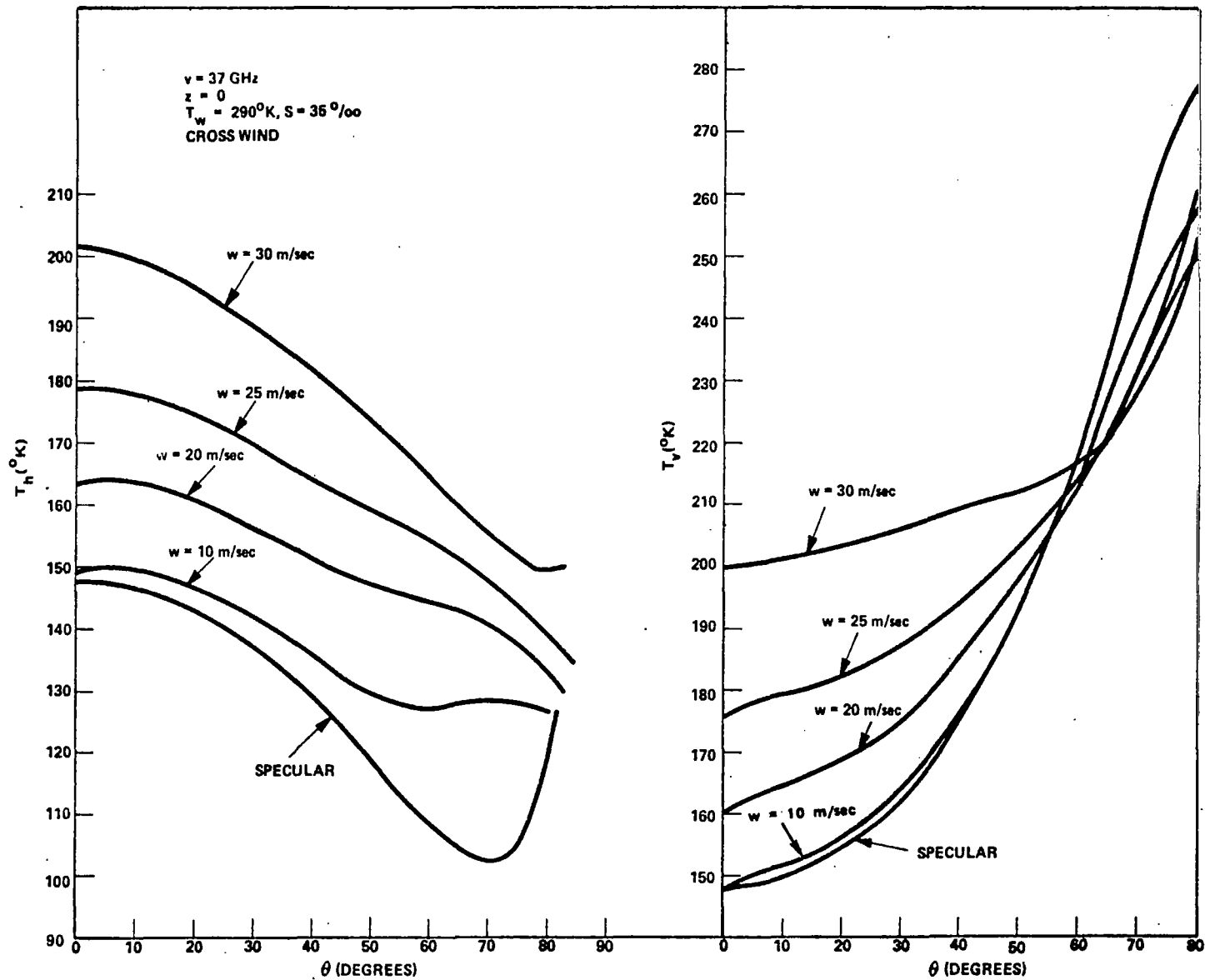
40

Figure 5. Horizontally and Vertically Polarized Brightness Temperatures
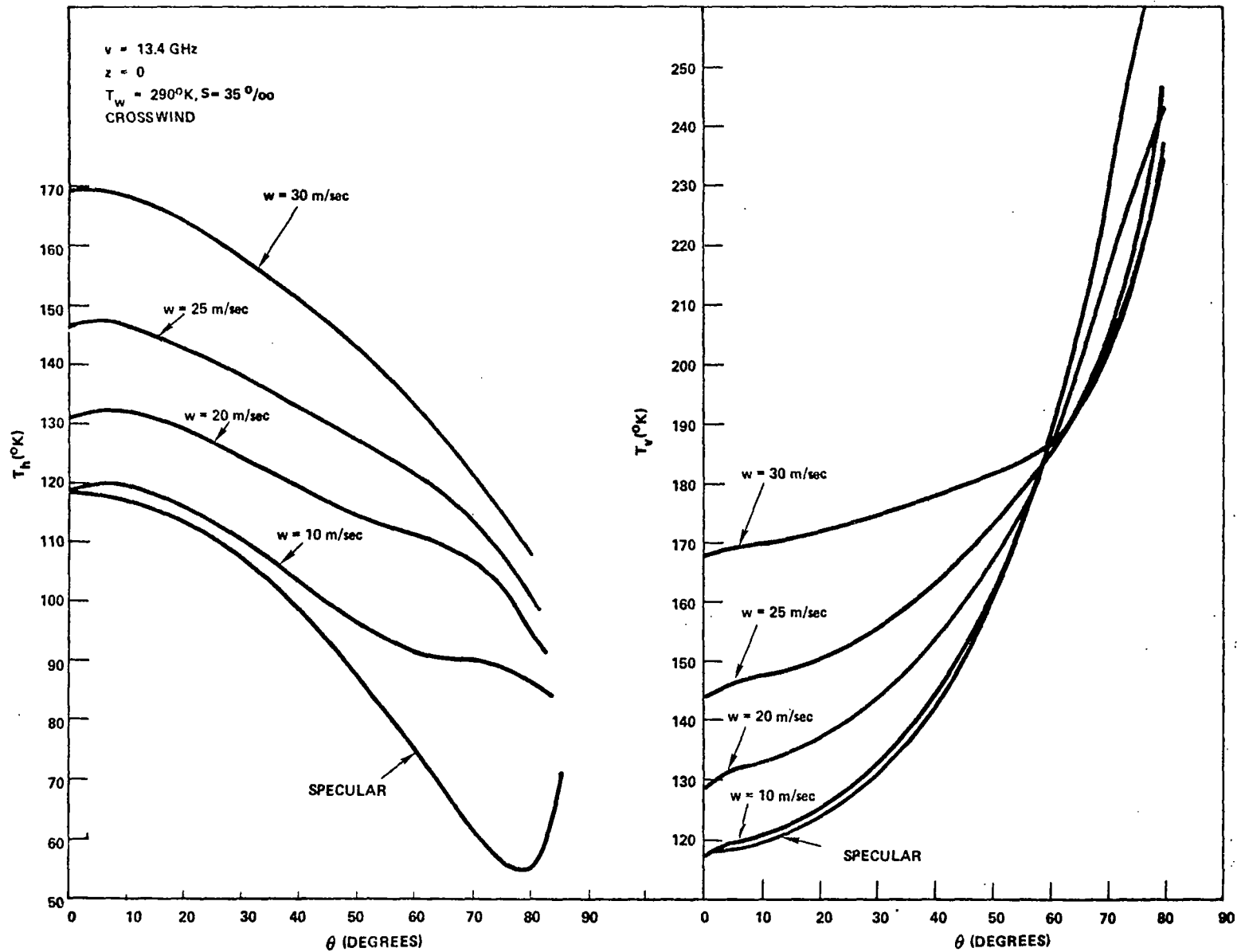at 37 GHz for Various Wind Speeds

Figure 6. Horizontally and Vertically Polarized Temperatures at 13.4 GHz
for Various Wind Speeds

42

has some influence. Note should also be made of the fact that the inclusion of foam in the computations has an influence on the "invariant angle" for vertical polarization. In fact, for very high wind speeds, the term invariant angle must be used somewhat loosely. However, for wind speeds less than 20 m/sec, the computations do show that at an angle near 55° the vertically polarized temperature is almost independent of the wind speed.

In order to more clearly illustrate some features relating to bright-ness temperature variations, it is useful to consider the data shown in Fig-ures 4 through 6 from another point of view. For example, Figure 7 is a plot of the brightness temperature increase of the sea over that of a reference specular surface as a function of wind speed for horizontal polarization and a frequency of 19.4 GHz. It is seen that the behavior of the curves at $\theta = 0^O$ differs considerably from that at $\theta = 50$ and 60°. At $\theta = 0^O$, brightness temperature variations are due principally to varying foam cover and conse-quently do not become large until the foam cover becomes significant. The situation is much different at $\theta = 50^O$. An immediate increase in the bright-ness temperature with wind speed is evident and is due to the ocean waves. The slight positive curvature, which is evident at high wind speeds, is caused by the foam. Finally, at $\theta = 60^O$, wave effects control the behavior of the brightness temperature curves until the wind exceeds 20 m/sec.

2.4   SUMMARY AND RECOMMENDATIONS FOR FUTURE RESEARCH

The numerical results presented in the previous section indicate that considerable progress has been achieved in understanding the physical basis for brightness temperature changes of the sea which arise from vary-ing oceanographic conditions. It is clear, however, that further theoretical studies and experimental measurements over a considerably wider range of conditions than are presently available are desirable.

The present studies have conclusively demonstrated that a com-prehensive grasp of the microwave emission properties of the sea can be achieved only by recognizing the distinct and different roles played by waves and foam. Thus, in addition to continuing with experiments in which a sea surface with both waves and foam is observed, future experimental measure-ments which are designed to obtain separate estimates of wave effects and
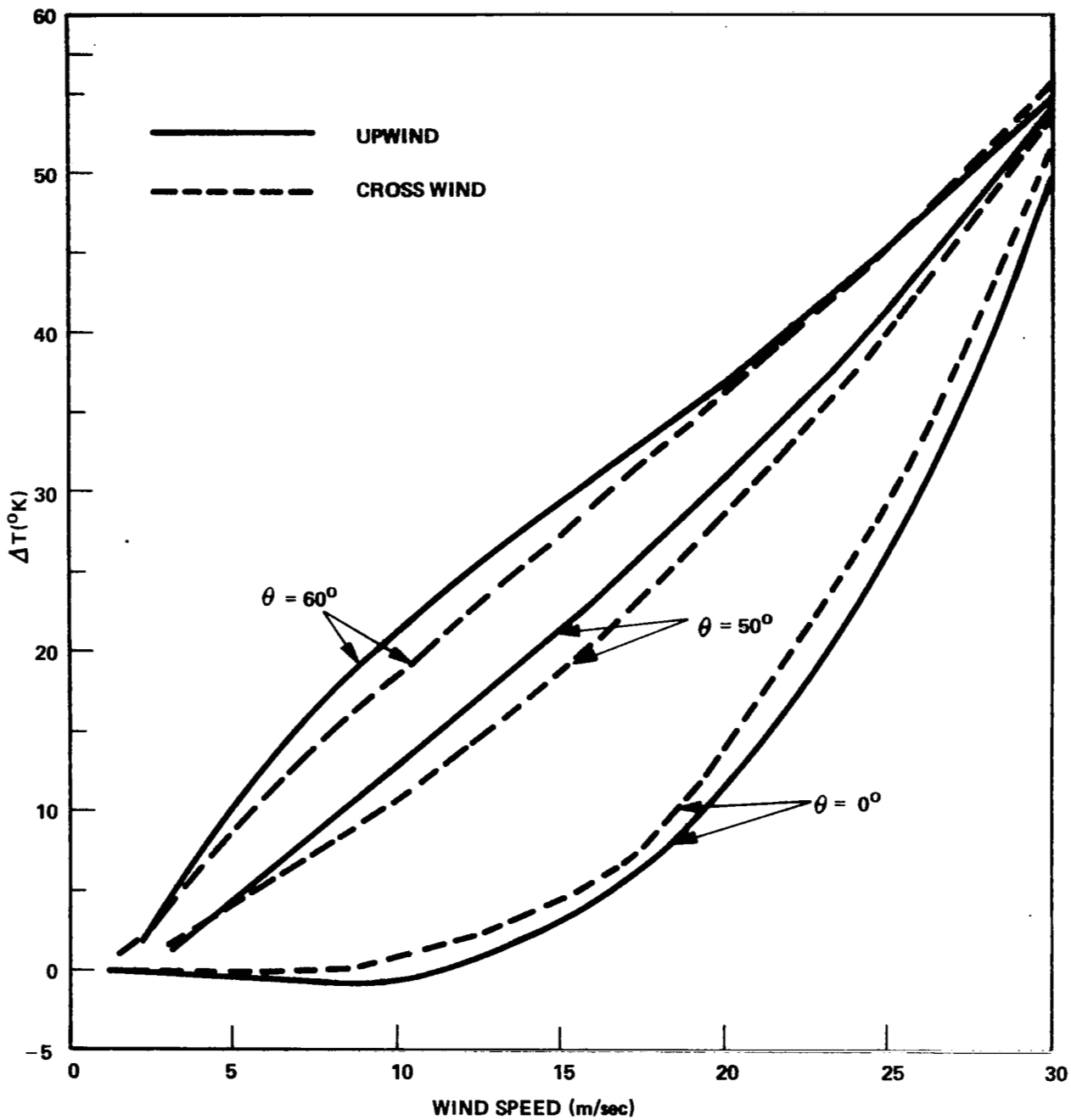
Figure 7. Increase in Horizontally Polarized Brightness
Temperature at 19.4 GHz

foam effects are needed in order to yield unambiguous results relating to these features. A useful start in this direction is represented by the work of Hollinger (Refs. 2 and 3) who has obtained data relating to a foam-free sea surface. However, since current studies indicate that an operational, satellite-borne radiometric system will probably make use of some frequencies above Hollinger's maximum of 19 GHz, measurements of the same nature in the neighborhood of 31 and 37 GHz are desirable. As is evident from the review of measurements relating to foam which was completed for the present study, much systematic work remains to be accomplished with regard to foam. In particular, brightness temperature measurements are needed at frequencies below 13 GHz. Further, the influence of the water temperature and salinity on the foam brightness temperature must be investigated. More carefully controlled experiments to reduce the scatter of the data relating to the angular dependence of the emissivity would also be desirable at all frequencies. Consideration should also be given to active as well as passive measurements on foam for much valuable information would be obtained from accurate measurements of its bistatic scattering cross sections.

From the point of view of theory, it is clear that progress in describing the scattering and emission properties of foam will be most difficult and, perhaps, theoretical considerations will be confined to the role of providing a general framework within which the experimental data are to be interpreted — for example, the choice of suitable functional forms for equations describing the emissivity and, if data becomes available, the scattering coefficients of foam. Far more can be expected with regard to the analysis of wave effects. The most obvious problem at the moment is the explanation of Hollinger's measurements which indicate that wave geometry effects tend to be less pronounced at low frequencies than at high frequencies. A possible mechanism and explanation for this effect may be contained in the two-scale model which was developed in the present study. However, confirmation must await further development of the computer program to yield numerical results.

The emphasis of the present study has been on factors relating to the sea itself as a source of brightness temperature variations. However,

for remote sensing applications, a description of brightness temperature variations due only to the sea is useless for it is known that large and important temperature changes may be produced by the atmosphere above the sea. Further, meteorological applications require information on both the atmosphere and sea state. Thus, little can be achieved with an operational system that cannot simultaneously obtain data relating to at least some atmospheric constituents (in particular, condensed water and water vapor) in addition to sea conditions. This important area has already received some attention among various groups studying the application of microwave radiometry. However, much remains to be done. In particular, the optimum choice of angle and, especially operational frequencies, taking into account the most recent results obtained with respect to emission from the sea, needs careful investigation in order to determine the accuracy with which atmospheric and sea state parameters may be deduced. In this regard, quantitative studies relating the absorption characteristics of various atmospheric constituents need to be stressed (qualitatively, and even semi-quantitatively, the main features of microwave absorption in the atmosphere may be considered known).

REFERENCES

(1) A. Stogryn, "The apparent temperature of the sea at microwave frequencies," IEEE Trans. on Antennas and Prop., vol AP-15, 1967, pp 278-286.

(2) J. Hollinger, "Passive microwave measurements of the sea surface," J. Geophys. Res., vol 75, 1970, pp 5209-5213.

(3) J. Hollinger, "Passive microwave measurements of sea surface roughness," IEEE Trans. Geoscience Electronics, vol GE-9, 1971, pp 165-169.

(4) W. Nordberg, J. Conaway, and P. Thaddeus, "Microwave observations of sea state from aircraft," Q. J. Royal Met. Soc., vol 95, 1969, pp 408-413.

(5) W. Nordberg, J. Conaway, D. Ross, and T. Wilheit, "Measurements of microwave emission from a foam covered, wind driven sea," J. Atmos. Sciences, vol 28, 1971, pp 429-435.

(6) G. Williams, "Microwave radiometry of the ocean and the possibility of marine wind velocity determination from satellite observations," J. Geophys. Res., vol 74, 1969, pp 4591-4594.

(7) A. Stogryn, "The emissivity of sea foam at microwave frequencies," to be published in J. Geophys. Res., March 1972. Also, see Appendix B of this report.

(8) A. Stogryn, "The effect of waves on the microwave brightness temperature of the sea," see Section 1 of this report.

(9) A. Stogryn, "Equations for calculating the dielectric constant of saline water," IEEE Trans. on Microwave Theory and Techniques, vol MTT-19, 1971, pp 733-736.

(10) D. Blanchard, "The electrification of the atmosphere by particles from bubbles in the sea." Progress in Oceanography, vol. 1, New York, Pergamon Press, 1963, pp 71-202.

(11) C. Rooth and G. Williams, "Microwave radiometry of the ocean," Quarterly Rept., University of Miami, Coral Gables, Fla., Aug 1970.

(12) E. Monahan, "Fresh water whitecaps," J. Atmos. Sci., vol 26, 1969, pp 1026-1029.

(13) E. Monahan, "Oceanic whitecaps," J. Physical Oceanography, vol 1, 1971, pp 139-144.

(14) D. Blanchard, "Whitecaps at sea," J. Atmos. Sci., vol 28, 1971, p. 645.

Appendix A

THE EMISSIVITY OF SEA FOAM AT MICROWAVE FREQUENCIES

Presently available evidence indicates that the two primary features of the ocean surface which are responsible for microwave brightness temperature departures from that characteristic of a specular surface are waves and foam. A theoretical treatment of wave effects has been given by Stogryn (Ref. 1) and has received partial confirmation in the experimental work of Hollinger (Refs. 2 and 3). Further work on the effect of waves is in progress and will be discussed elsewhere. The significance of foam on the water's surface seems to have first been recognized by Williams (Ref. 4) and several subsequent experiments performed by various groups have verified its importance. Although an interesting attempt at a theoretical description of the emissivity of foam was made by Droppleman (Ref. 5), it is clear that the complexity of the electromagnetic boundary value problem has precluded the construction of a physically and mathematically convincing theoretical model. Thus, at least for the present, complete reliance must be placed on experimental data in studies relating to the effects of foam.

To date, the published data on the microwave radiometric properties of foam has been quite sparse and no attempt seems to have been made to correlate the various measurements which are available. In view of the importance of this problem in connection with the interpretation of many proposed remote sensing experiments, a synthesis of known data is attempted in this work.

A. 1   SOME BASIC RELATIONSHIPS

The brightness temperature $T_p(\nu, \theta)$ of radiation with polarization p and frequency ν propagating away from the surface S (see Figure A-1) may be expressed as

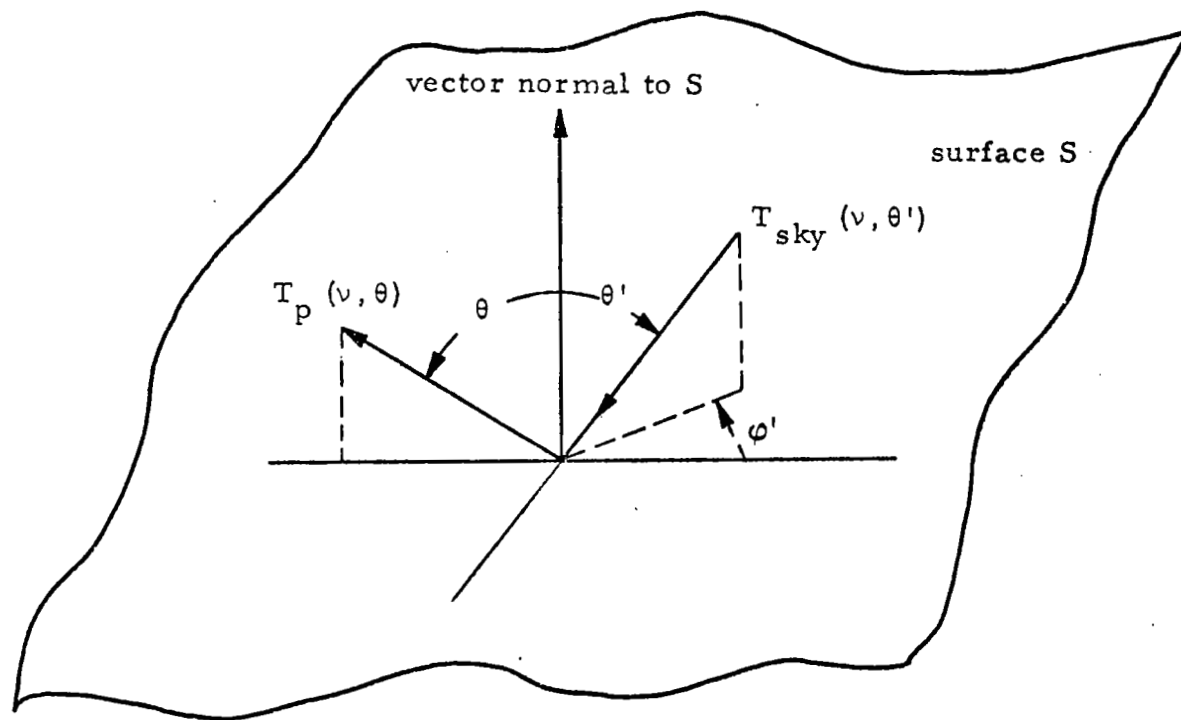$$T_p(\nu, \theta) = \epsilon_p(\nu, \theta) T_w + T_p^r(\nu, \theta) \tag{A-1}$$

Figure A-1. Geometry for Determining Emissivity

where $\epsilon_p(\nu, \theta)$ is the emissivity in the direction θ, T_w the thermal temperature of the water and foam, and $T_p^r(\nu, \theta)$ the temperature of the reflected sky radiation. In writing (A-1), it is assumed that the brightness temperature is measured near the surface so that certain additional atmospheric contributions to $T_p(\nu, \theta)$, which are sometimes of importance, may be ignored. Further, an implicit assumption is made that azimuthal variations in the incident sky brightness temperatures and emissivity can be ignored. This hypothesis seems to be quite reasonable for sea foam since foam generally has a statistically isotropic structure and, for the data to be discussed below, atmospheric conditions also appeared to be isotropic.

As is customary in microwave radiometric studies, the two independent polarization directions p will be taken to be horizontal (h) and vertical (v). Peake (Ref. 6) has shown that the term $T_p^r(\nu, \theta)$ in (A-1) may be expressed by means of a set of bistatic scattering coefficients $\gamma_{ij}(\nu; \theta, ; \theta', \varphi')$ (i, j = h or v) in the form

$$ T_p^r(\nu, \theta) = \frac{1}{4\pi} \int \left[\gamma_{ph} + \gamma_{pv} \right] T_{sky}(\nu, \theta') \sin\theta' \, d\theta' \, d\varphi' \quad (p = h \text{ or } v) $$

(A-2)

where T_{sky} is the incident sky brightness temperature. Further, the same scattering coefficients are closely related to the emissivity by the equation

$$ \epsilon_p(\nu, \theta) = 1 - \frac{1}{4\pi} \int \left[\gamma_{ph} + \gamma_{pv} \right] \sin\theta' \, d\theta' \, d\varphi' \quad (p = h \text{ or } v) $$

(A-3)

The above formulation shows that a complete description of the microwave properties of foam is contained in the scattering coefficients γ_{ij}. Thus, either active (scattering) measurements or passive (radiometric) measurements may be used in principle to deduce the emissivity of foam. Scattering experiments to determine γ_{ij} as a function of both the incident and scattering angles have the further advantage of providing an accurate means for calculating the reflected contribution to $T_p(\nu, \theta)$. However, currently available information is far from adequate to determine

A-3

the form of these coefficients. In fact, in order to interpret the radio-
metric data to be discussed below, recourse to the simplest possible
hypothesis, namely, that the angular dependence of γ_{ij} contains a delta
function part of the form $\delta(\theta - \theta')\delta(\varphi')$, will be made. In this approxi-
mation, (A-1) reduces to

$$T_p(\nu, \theta) = \epsilon_p T_w + \left[1 - \epsilon_p\right] T_{sky}(\nu, \theta) \qquad (p = h \text{ or } v) \qquad \text{(A-4)}$$

The use of (A-4), while not exact, will allow at least a first order correc-
tion for sky temperature effects to be applied to the data. This correction
is most important at large angles of observation.

Before proceeding to a discussion of the data, it will be reiter-
ated that the aim of this study is the specification of the properties of a
water surface covered completely with foam. Thus, in analyzing some
measurements which were obtained over surfaces only partially foam
covered, it was necessary to assume that the total brightness temperature
may be decomposed into

$$T_p = (1 - f)(T_p)_w + f(T_p)_f \qquad \text{(A-5)}$$

where f is the fractional foam coverage, $(T_p)_w$ is the brightness temper-
ature due to a foam-free water surface, and $(T_p)_f$ is the brightness tem-
perature due to a 100 percent foam covered surface. The assumptions
under which (A-5) holds are quite mild and do not impose any practical
restrictions for typical operational conditions. Conversely, in applying
the results obtained below to actual experiments, (A-5) must be taken into
account since water surfaces are generally completely foam covered only
in exceptional circumstances.

Data obtained by passive and active electromagnetic experiments
are discussed separately below.

A.2   PASSIVE MEASUREMENTS

A list of measurements on foam which are known to the author is shown in Table A-1. Unfortunately, all of the reported data was not found to be suitable for quantitative comparisons. Two primary considerations determined the choice of data which was analyzed. First, was the availability of information relating to the absolute calibration of the radiometers. This is a critical factor in any comparison because absolute calibration errors greater than $70^{\circ}K$ are apparent in some cases. A neglect of such brightness temperature shifts can obviously conceal any correlations which may exist. Secondly, the foam cover on the water surface was required. For surfaces with 100 percent foam cover, this does not present any difficulty. On the other hand, it appears that the determination of foam coverage from optical photographs can be quite subjective and uncertain when the foam cover is small (even when there is a clearly established brightness temperature change). Thus, the error in extrapolating such results to 100 percent coverage may be quite large. For this reason, cases exhibiting complete foam coverage were preferred and, in fact, only one example with less foam was used in establishing the basic form of the emissivity curves.

The data in Edgerton, et al (Ref. 7) at 37 GHz provides an illustration of the brightness temperature characteristics of foam. Figure A-2 is a plot of the scan over the surf zone taken at Newport Beach, California. The data for $5 < \theta < 90^{\circ}$ refer to the foam while for angles greater 90°, the radiometer observed the sky temperature ($\theta = 180^{\circ}$ corresponds to zenith). The latter data is important for checking the absolute calibration of the radiometer. Large fluctuations in the brightness temperature are evident in the figure and are ascribed to the constantly changing foam coverage as well as to breaking waves which have the effect of changing the local angle of incidence θ. Although the magnitude of the brightness temperature for horizontal polarization differs markedly from that of a smooth surfaced water body, it is interesting to note the same qualitative decrease in temperature with increasing angle which is characteristic of all specular surfaces out to angles where the sky temperature dominates ($\theta \geq 80^{\circ}$). The vertically polarized temperature behaves quite differently. Instead of

Table A-1

REPORTED RADIOMETRIC MEASUREMENTS ON FOAM

| Reference	Frequency (GHz)	Polarization	Angle (degrees)	Foam Cover (%)	Remarks
Edgerton, et al, Reference 7	13.4, 37	h and v	20	100	Artifically generated foam in a large tank of water (salinity = 33 ^{o}/oo) T_w = 295°K
	13.4, 37	h and v	50	100	Measured in surf zone at beach. Wave height < 1 ft. $T_w \approx$ 286°K
	37	h and v	5<θ<90	~100	Scan over surf zone near shore at Newport Beach, Calif. Considerable fluctuations due to variable foam cover and breaking waves. T_w = 288°K
Hollinger, Reference 2	8.36, 19.34	h and v	20<θ<55	?	Natural and artifically generated foam observed at Argus Island. Obtained lower bounds to foam effects.
Nordberg, et al, Reference 8	19.4	h	0	?	Measurement over Salton Sea. T_w = 294°K. Wind speed ~ 15 m/sec
	19.4	h	0	0-100	Flights over North Atlantic Ocean and North Sea.
Nordberg, et al, Reference 9	19.4	h	0<θ≤70	~25	Flight over North Sea. T_w = 277°K, wind speed = 25 m/sec (case F in reference)
Williams, Reference 4	9.4, 15.8, 22.2, 34	?	20°	100	Artificially generated foam in tank of water. Radiometer calibrations not established. Antenna pattern effects also present in data. Some data relating to Hurricane Beulah (1967)
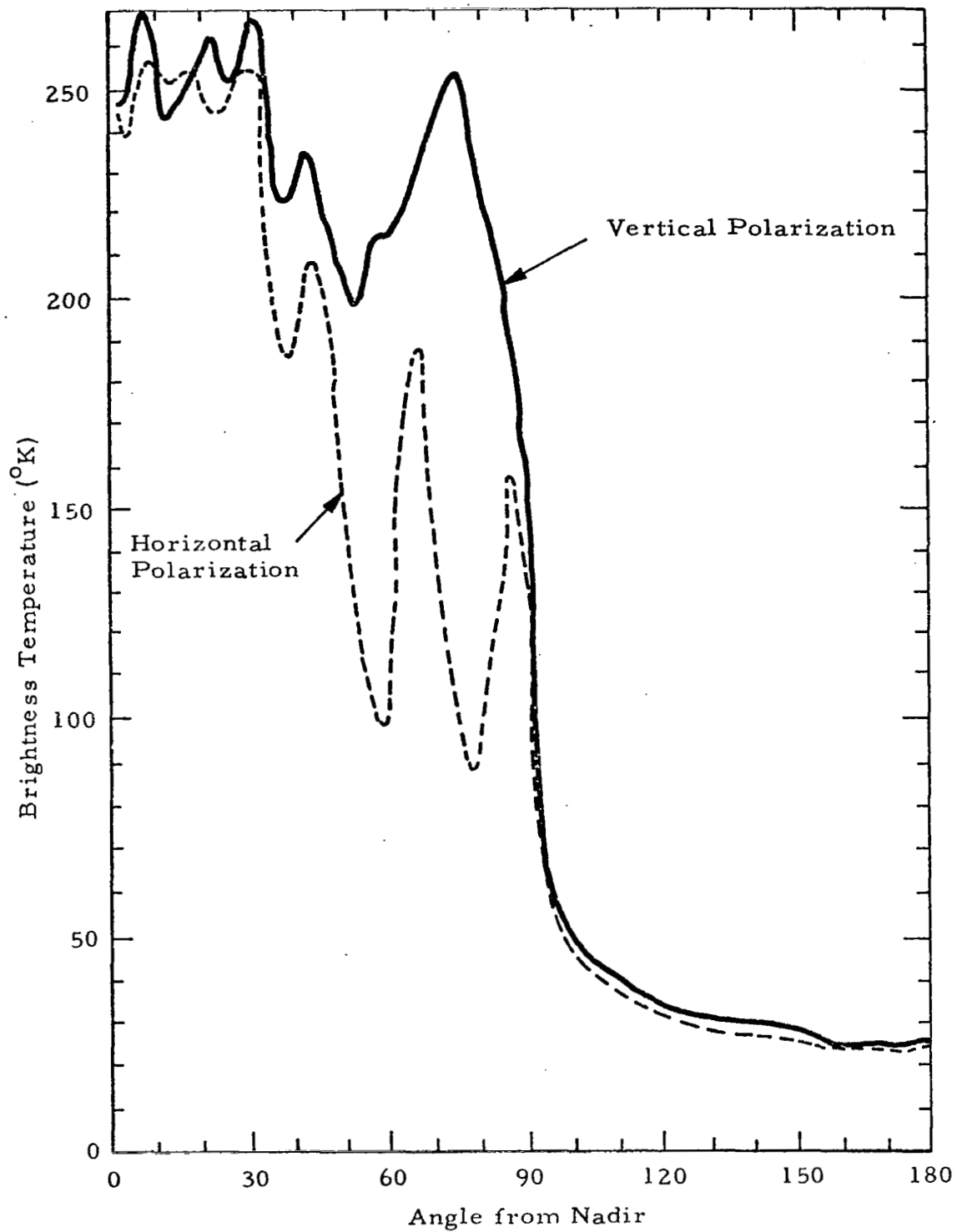
Figure A-2. Brightness Temperature of Surf Zone at 37 GHz

increasing with increasing θ, as is typical of specular surfaces for angles less than the Brewster angle, the brightness temperature is seen to generally decrease until $\theta = 55^O$ from which point it increases up to an angle not too different from the Brewster angle of a smooth surfaced body of water. It is also interesting to observe that foam differs considerably from examples of very rough surfaces that have been discussed in the literature. In particular (Refs. 6 and 10), it is known that surfaces covered with vegetation such as grass and weeds tend to exhibit the same behavior for both horizontal and vertical polarization and no Brewster angle effects are observed.

The data in Figure A-2 represents the only information on the brightness temperature of foam for vertical polarization known to the author which covers angles greater than $\theta = 55^O$. For this reason, the interesting behavior at large angles which is observed here will not be supported by other direct evidence although tentative confirmation is provided by some scattering data to be discussed below.

In order to convert the measurements exhibited in Figure A-2 into emissivity data, the absolute calibration must be established and sky temperature effects extracted. In this example, the measured sky temperatures are consistent with known atmospheric conditions prevailing at the time of the experiment and the difference between the measured sky temperatures as the radiometer was switched between the vertical and horizontal polarization modes is sufficiently small so as to establish some confidence in the calibration. Thus, using the known water temperature $T_w = 288^O K$ and (A-4), it is possible to compute ϵ_p (p = h or v) or, equivalently, the product $\epsilon_p T_w$. The latter quantity seems to be a better parameter to use at this time because the different experiments which will be compared were performed at different water temperatures. If the hypothesis is made that $\epsilon_p T_w$ for foam behaves in the same way with T_w as for water in bulk form, then $\epsilon_p T_w$ should be rather insensitive to the water temperature in the frequency range to be considered (Ref. 1). Results, after performing a partially subjective smoothing of the data in order to eliminate the effects of varying foam coverage and breaking waves which were mentioned above, are shown in Figure A-3.
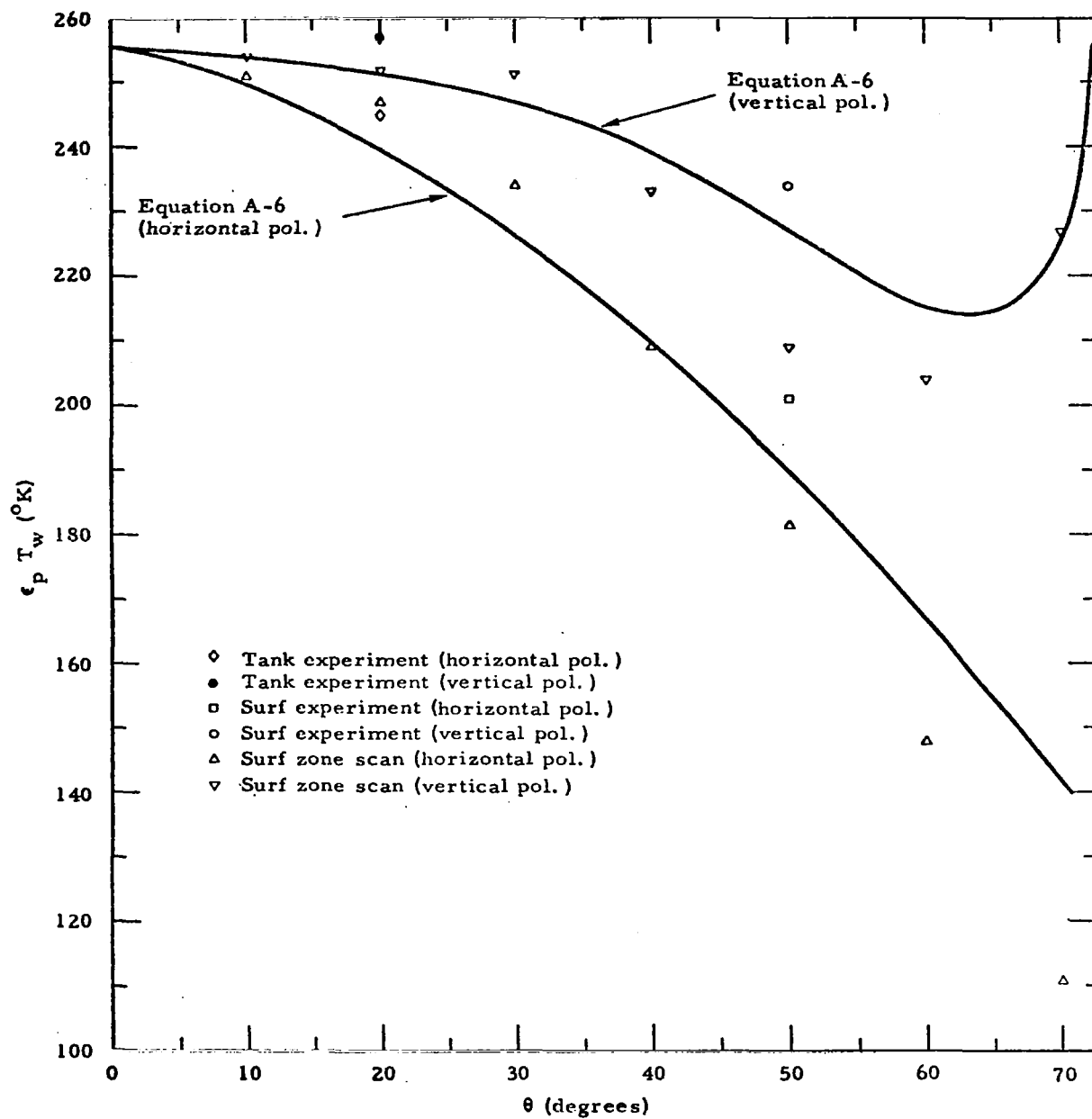
Figure A-3. Emitted Temperature of Foam at
37 GHz

The results of other measurements at 37 GHz (Ref. 7) are also shown in Figure A-3. The tank experiment resulted in a temperature increase of 104°K for horizontal polarization and 104°K for vertical polarization over that of a specular water surface. The calibration check over a specular water surface which was made during the experiment resulted in a temperature of 134°K for horizontal polarization which is 11°K lower than a calculation with a realistic model atmosphere yielded. Since the properties of a smooth water surface can be calculated with high accuracy, it was assumed that an absolute calibration error of 11°K existed in the horizontally polarized data. After applying the calibration data as well as extracting the effect of the incident sky temperature, $\epsilon_h T_w$ was found to be 245°K for foam. A similar treatment of the vertically polarized data showed a calibration error of 18°K and resulted in $\epsilon_v T_w = 257^{\circ}$K. It is apparent that although the foam in the tank was generated artificially by blowing air through the water, the results are entirely consistent with those obtained at Newport Beach. The surf zone data at $\theta = 50^{\circ}$ was treated in a similar manner and yields corrected estimates of 201°K and 234°K for $\epsilon_h T_w$ and $\epsilon_v T_w$ respectively.

Data from Edgerton, et al (Ref. 7) at 13.4 GHz, after calibration and sky temperature corrections are shown in Figure A-4.

The experiments of Nordberg, et al (Ref. 9) at 19.4 GHz were performed for horizontal polarization only. The authors estimated an absolute calibration error in the range 10 to 15°K. On the basis of a comparison of their computed smooth sea curve and their Case B, a calibration error of 15°K will be assumed here. A model atmosphere which produces a zenith sky temperature of 19°K at 19.4 GHz is consistent with the atmospheric effects described in the reference for $\theta = 0$ and provides the basis for making atmospheric corrections at other angles. Two measurements are of particular interest here. The first was an observation of a large foam patch which filled the radiometer beam at $\theta = 0^{\circ}$ and resulted in a temperature of 220°K. After applying the above-mentioned calibration correction and extracting a small sky temperature contribution, it is found that $\epsilon_h T_w = \epsilon_v T_w = 232^{\circ}$K at $\theta = 0^{\circ}$. The second measurement which will be considered here is a scan over the range $0 < \theta < 80^{\circ}$ (Case F of Reference 9).
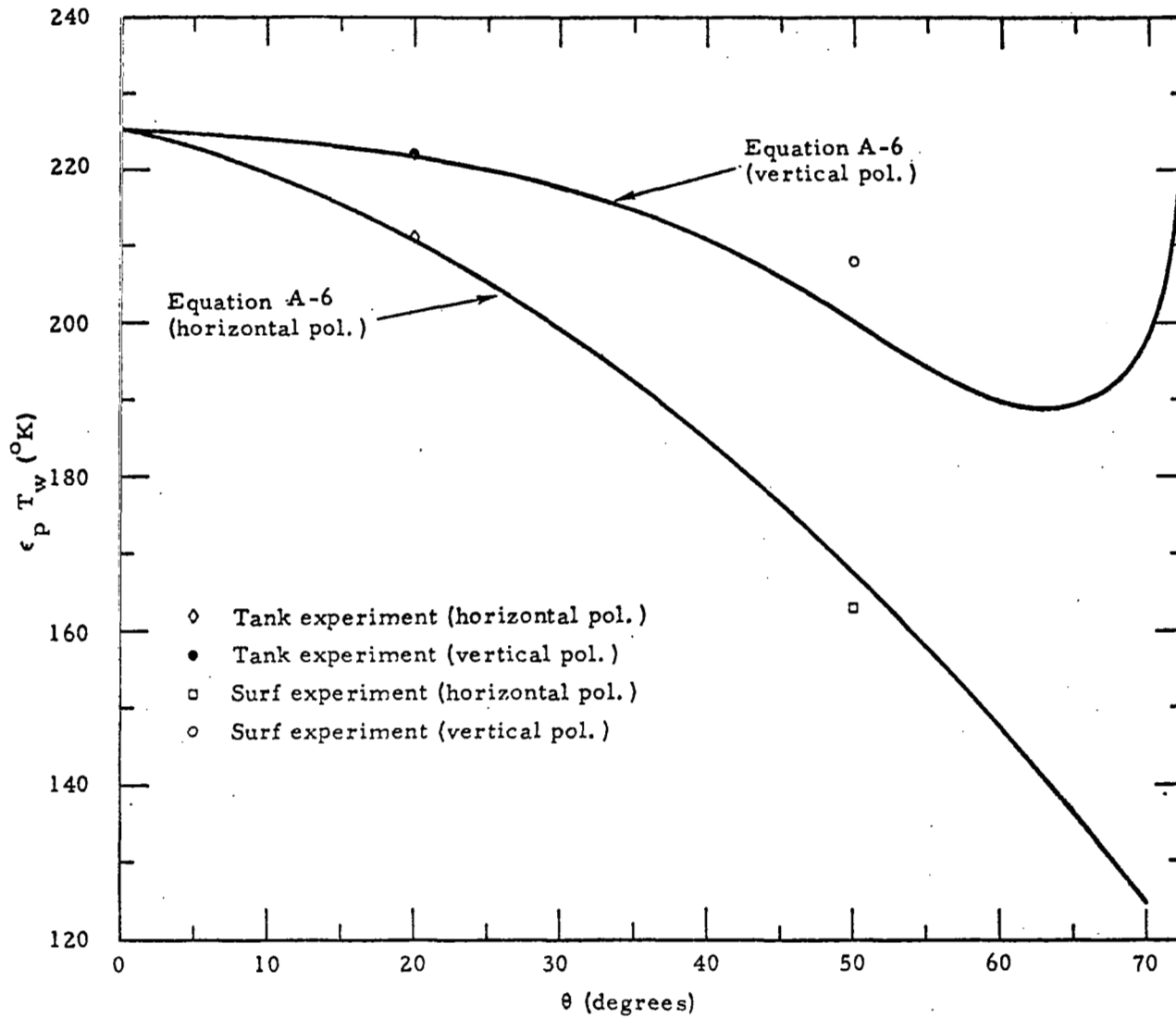
Figure A-4. Emitted Temperature of Foam at 13.4 GHz

Although the foam cover was far less than 100 percent for this case, it warrants attention because it provides data on angular variations at 19.4 GHz. Several interesting questions relating to the interpretation of wave effects also arise in connection with this example.

In order to determine the emissivity of the foam at 19.4 GHz from the Case F curve in Reference 9, it is necessary to estimate the foam coverage and deviations in the brightness temperature from a specular surface due to the waves on the sea surface. The foam coverage was determined by means of (A-5) in connection with the (corrected) measured temperatures of 132°K and 157°K at $\theta = 0$ for Cases B and F, respectively of the reference. Assuming that the difference between these cases is entirely due to foam (see remarks below), it is found that $f = 0.243$ if use is made of the measured increase of 103°K for a 100 percent foam covered surface. This estimate falls precisely on the dotted curve shown in Figure 5 of Reference 9, and, of course, is not compatible with the possible alternate curve discussed in the reference. The assumption that the brightness temperature at $\theta = 0$ is the same as that for a smooth sea surface for Case B and for the non-foam part of the temperature contribution to Case F is consistent with both the theoretical results of Stogryn (Ref. 1) and the observation of Nordberg, et al (Ref. 9) that at $\theta = 0$ and wind speeds less than 7 m/sec (in which case foam coverage is nil) no brightness temperature increase over that of a specular surface occurs.

At angles of incidence other than $\theta = 0^\circ$, an allowance for wave effects must be made in interpreting the data of Case F. The measurements of Hollinger (Ref. 3) show that the product $\epsilon_h T_w$ at 19.4 GHz increases at approximately the rate $0.05 + 0.0175\theta$ $^\circ$K per m/sec wind speed for $30 < \theta < 70^\circ$. Although the maximum wind speed on which this rate was based was 15 m/sec, an extrapolation to the 25 m/sec speed applicable to Case F was made. Hence, the product $\epsilon_h T_w$ for the foam-free contribution to the brightness temperature was calculated on the basis of the specular surface result plus an additional term equal to $1.25 + 0.4375\theta$ $^\circ$K. Although there is some deviation from Hollinger's data for angles less than 30°, the linear dependence of the additional term with θ was assumed to hold

for all angles. Such an approach leads to only a small wind speed dependence at $\theta = 0$ and is consistent with the assumptions made in the previous paragraph.

Figure A-5 shows the resultant product $\epsilon_h T_w$ for a 100 percent foam-covered surface at 19.4 GHz when the data of Nordberg, et al (Ref. 9) is analyzed in the manner discussed above. It is important to note that $\epsilon_h T_w$ decreases with increasing angle in a manner similar to that observed at 13.4 and 37 GHz. If the effects of waves had not been extracted from the measured data, a substantial increase in $\epsilon_h T_w$ would have been obtained with increasing angle (approximately 18°K between $\theta = 0$ and 60°), thus implying an anomalous behavior at 19.4 GHz. This indirect evidence, together with the direct evidence of Hollinger (Refs. 2 and 3) on the temperature effects of waves, demonstrates the untenability of the contention of Nordberg, et al (Ref. 9) that the effect of wave slope geometry is negligible when foam cover is not total. At sufficiently large angles, wave structure cannot be ignored. For θ near zero, of course, wave geometry effects are considerably reduced in magnitude and foam, when it exists on the water surface, may easily produce the dominant effect.

In order to correlate the data shown in Figures A-3 - A-5 and to provide a means for extrapolating to other frequencies, it is desirable to fit the data with a simple analytic expression. The functional form

$$\epsilon_p(\nu, \theta) T_w = \epsilon(\nu, 0) \, T_w F_p(\theta) \qquad\qquad (p = h \text{ or } v) \qquad (A\text{-}6a)$$

was chosen in analogy with the known behavior of the emissivity of a smooth water surface. That is, to within an accuracy of a few percent in the range $5 < \nu < 50$ GHz, computations show that ϵ_h and ϵ_v for the specular case may be approximated as functions of angle only times a function of frequency only. In fitting the form (A-6a) to the data, the constraint $\epsilon_h T_w = \epsilon_v T_w$ at $\theta = 0$ was imposed because of the isotropy of the foam. It was found that
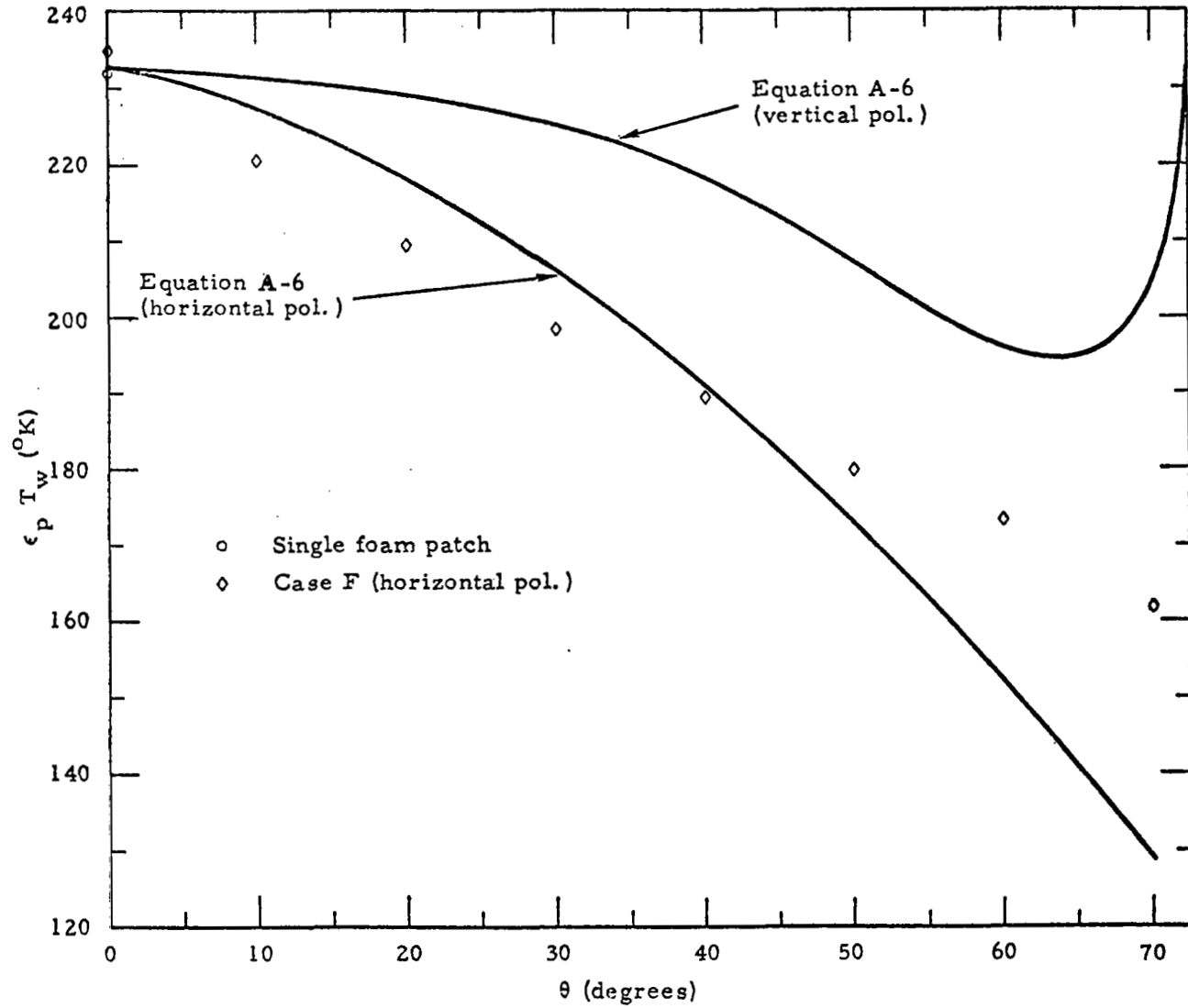
Figure A-5. Emitted Temperature of Foam at 19.4 GHz

$$\epsilon(\nu, 0) T_w = 208 + 1.29 \nu \quad ^{\circ}K \tag{A-6b}$$

$$F_h(\theta) = 1 - 1.748 \times 10^{-3}\theta - 7.336 \times 10^{-5}\theta^2 + 1.044 \times 10^{-7}\theta^3 \tag{A-6c}$$

$$F_v(\theta) = 1 - 9.946 \times 10^{-4}\theta + 3.218 \times 10^{-5}\theta^2$$
$$- 1.187 \times 10^{-6}\theta^3 + 7 \times 10^{-20}\theta^{10} \tag{A-6d}$$

where ν is expressed in GHz and θ in degrees. The curve fits were performed in the angular range $0 \leq \theta \leq 70^{\circ}$. Computations based on (A-6) are shown in Figures A-3, A-4 and A-5. It is believed that the analytical results fall within the uncertainties in the experimental data. The largest deviations between the analytic results and various data points occur at large angles. However, it is precisely in this region that the possibility of cumulative errors in the treatment of the data was greatest. The advantage of working primarily with data obtained from 100 percent foam covered surfaces is apparent at this point. If the analytical results are applied to partially foam covered surfaces, absolute errors are reduced by a factor f.

It is interesting to observe that the frequency dependent part of (A-6) is well represented by a linear function in the range $13.4 < \nu < 37$ GHz. Exact calculations for a smooth water surface also show an almost linear dependence of the emissivity on frequency in this range but with a rate of increase approximately 29 percent smaller than that given by (A-6b) for foam. In particular, these results imply that the increase in the brightness temperature of foam over that of a specular surface is roughly $3^{\circ}K$ greater at 19.34 GHz than at 8.36 GHz for $\theta = 0^{\circ}$ (less at higher angles). This is in accord with the observation of Hollinger (Ref. 2) who found the same increase at 8.36 and 19.34 GHz within his measurement error of about 20 percent.

A.3 ACTIVE MEASUREMENTS

No measurements of the scattering coefficients of naturally occurring foam appear to have been made. Information based on active

measurements is limited to that obtained from small scale laboratory simu-
lation experiments and, to date, is very restricted in scope.

Two types of experiments have been reported by Rooth and
Williams (Ref. 11) at a frequency of 9.8 GHz. One consisted of measuring
the reflection coefficient of foam produced from soapy water in a small (2.5-
foot diameter) wading pool. The transmitting and receiving horns each had
a half-power beamwidth of 17° and measurements were conducted slightly
beyond the near fields of the horns. Only results for vertical polarization
were obtained and these primarily for the case in which both the angle of
incidence and reflection were 7°. Several different bubble sizes were
investigated as well as the effect of varying the foam thickness. Upon iden-
tifying the integral term of (A-3) with the measured reflection coefficient,
emissivities varying from 0.44 (single layer of 0.5-mm diameter bubbles)
to nearly 1 (1-cm thick foam layer) were found. Attempts to measure radi-
ation scattered at angles differing from the incidence angle were unsuccess-
ful. Similar results were obtained at an angle of incidence of 45°. The
second type of experiment discussed by Rooth and Williams consisted of a
reflection measurement using a slotted waveguide terminated with a 2-mm
layer of foam on water. A reflection coefficient of 0.027 which, with the
same assumption as above, yields an emissivity of 0.973 was found. This
value agrees poorly with the passive emissivity measurements discussed in
the previous section.

The only other known active measurements relating to foam were
kindly performed by Mr. G. Poe for the author. Measurements of the
reflection coefficient were performed with the Aerojet-General ellipsom-
eter at a frequency of 37 GHz using a small tray of water at a temperature
of 295^OK. The water surface was covered by 5 mm of foam consisting of
soap bubbles ranging from 0.1 to 2 mm in diameter with an average size
estimated to be 0.5 mm. Measurements were made at angles of 30, 40 and
50° keeping the angle of incidence equal to the angle of reflection. Hori-
zontal or vertical polarization could be chosen independently for both the
transmitted and received wave. The magnitude of the cross polarized
received power from foam was found to be more than 50 dB below that
received with uncrossed polarization from a reference metal plate. Hence,

at least for $\theta \approx \theta'$ and $\varphi \approx 0$, one can conclude that the scattering coefficients γ_{hv} and γ_{vh} are extremely small. For uncrossed polarizations, the reflection coefficients were found to be 0.130, 0.163, and 0.203 for horizontal polarization and 0.65, 0.040, and 0.010 for vertical polarization at angles of 30, 40 and 50° respectively. Neither of these sets of numbers yield emissivities (assumed approximately equal to one minus the reflectivity) in quantitative agreement with the passive measurements. Several explanations are possible. The first is that the foam made from soap has different properties from natural sea foam (bubble size distribution, thickness, etc.) so that only qualitative comparisons should be made. A second possibility is that a significant amount of energy was scattered away from the specular direction (the half power antenna beamwidths were approximately 5°), thus invalidating the assumed relation between the emissivity and the reflection coefficient. In fact, if it is assumed that the integral term in (A-3) has a value 50 percent greater than the measured reflectivities, the horizontally polarized data yields values of $\epsilon_h T_w$ of 234, 218, and 199°K at angles 30, 40 and 50° respectively. This is in agreement with the passive emissivity data. A 50 percent correction does not result in adequate agreement with the passive measurements when applied to the vertically polarized data. However, the angular range over which γ_{vv} has significant values does not necessarily coincide with that of γ_{hh} . A further discrepancy arising with the vertically polarized data is that the reflectivity is monotonically decreasing with increasing angle which implies a monotone increase in the emissivity. The increase is consistent with the increase observed with the passively obtained data at large angles but contradicts the behavior observed with this data for smaller angles at both 37 and 13.4 GHz.

Since it is possible to choose the angle of the receiving antenna to be different than that of the transmitting antenna in the ellipsometer, an attempt was made to obtain information for vertical polarization when the angles of incidence and scattering differed. Although a slight difference in the form of the scattering curve for foam compared to that of a reference metal plate was obtained, the difference was not great enough to allow a quantitative distinction to be made between possible non-specular scattering and the effects of the finite antenna beamwidths.

Because of the limited data and gross nature of the hypotheses which are required to convert the reflection measurements to emissivities and because of possible structural differences between natural foam and foam made from soapy water, the scattering measurements which have been discussed do not appear to be as reliable quantitative guides to the emissivity of sea foam as the passive measurements. However, they do indicate some qualitative features which can validly be extrapolated to natural foam. In particular, it is probably correct to assume that the scattering coefficients have substantial values only for θ' differing from θ by less than 10° and that the cross terms γ_{hv} and γ_{vh} are small compared to γ_{hh} and γ_{vv} in this angular region.

A.4 CONCLUSIONS

A consistent picture of the emissivity characteristics of sea foam at microwave frequencies, which is summarized by the set of equations (A-6), has resulted from the analysis of available radiometric data. Although based on data obtained in the frequency range $13.4 \le \nu \le 37$ GHz, it is believed that an extrapolation to the range $3 \le \nu \le 50$ GHz is valid.

Presently available information on the scattering properties of foam is far less extensive than desirable for quantitative applications to radiometric problems. While it is in partial qualitative agreement with the radiometric data, quantitative agreement is lacking. Considerably more confidence is placed in the radiometric data than in the deductions based on the presently available scattering measurements.

REFERENCES

(1) Stogryn, A., "The apparent temperature of the sea at microwave frequencies," IEEE Trans. Antennas and Propag. AP-15, 278, 1967.

(2) Hollinger, J., "Passive microwave measurements of the sea surface," J. Geophys. Res. 75 (27), 5209, 1970.

(3) Hollinger, J., "Passive microwave measurements of sea surface roughness," IEEE Trans. Geoscience Electronics, GE-9, 165, 1971.

(4) Williams, G., "Microwave Radiometry of the ocean and the possibility of marine wind velocity determination from satellite observations, J. Geophys. Res., 74 (18), 4591, 1969.

(5) Droppleman, J., "Apparent microwave emissivity of sea foam," J. Geophys. Res. 75 (3), 696, 1970.

(6) Peake, W., "Interaction of electromagnetic waves with some natural surfaces," IRE Trans. Antennas and Propag. (Special Supplement) 7, S324, 1959.

(7) Edgerton, A., D. Trexler, G. Poe, A. Stogryn, S. Sakamoto, J. Jenkins, D. Meeks, and F. Soltis, "Passive microwave measurements of snow, soils and oceanographic phenomena," Aerojet-General Corp. Tech. Rep. No. 6 SD 9016-16, Feb. 1970.

(8) Nordberg, W., J. Conaway, and P. Thaddeus, "Microwave observations of sea state from aircraft," Q. J. Royal Met. Soc. 95, 408, 1969.

(9) Nordberg, W., J. Conaway, D. Ross and T. Wilheit, "Measurements of microwave emission from a foam covered, wind driven sea," J. Atmos. Sciences, 28, 429, 1971.

(10) Chen, S., and W. Peake, "Apparent temperatures of smooth and rough terrain," IRE Trans. Antennas and Propag. 9, 567, 1961.

(11) Rooth, C. and G. Williams, "Microwave radiometry of the ocean," University of Miami, Quarterly Reports, May and Aug. 1970.

Appendix B

THE EFFECT OF THE OCEAN'S THERMAL BOUNDARY LAYER
ON MICROWAVE BRIGHTNESS TEMPERATURES

A measurement of the temperature gradient which is known to exist in the upper millimeter of the ocean's surface layer (Ref. 1) can provide important information relating to the heat balance of the ocean. Experiments using infrared radiometers for this purpose have been performed by Ball (Ref. 2) and McAlister (Ref. 3) on a local basis but global measurements, such as can be obtained by satellite-mounted instruments, seem to be less feasible. The primary difficulty appears to be associated with atmospheric absorption in the infrared region of the spectrum and, in particular, the perturbing influence of cloud cover which exists over large portions of the sea's surface. For this reason, McAlister (Ref. 4) has suggested the application of microwave radiometers which, in appropriate frequency bands, are far less sensitive to atmospheric conditions than infrared instruments, for temperature gradient determinations. However, estimates of the magnitude of the brightness temperature changes at microwave frequencies due to the thermal boundary layer have not been published and hence the utility of the microwave experiment not established. It is the purpose of this communication to provide a quantitative indication of the effects involved.

The computations to be discussed below are based on an idealized model in which the sea surface is assumed to be perfectly smooth. Under such conditions, it is known (Ref. 5) that the temperature in the surface layer differs from the bulk temperature in an approximately exponential manner with depth. Thus, measuring the depth z downward from the surface, the water temperature $T(z)$ may be expressed as

$$T(z) = T_w + \delta T \exp(-z/d) \qquad \text{(B-1)}$$

where T_w is the bulk temperature and δT and d are constants depending on local environmental conditions. Measurements (Refs. 2, 3, 6) have

shown that δT may vary in the range $-1.5 \leq \delta T \leq 1.5^{\circ}C$. However, under the usual conditions prevailing near the ocean's surface, $\delta T \simeq -0.25^{\circ}C$ is typical. The data of Spangenberg and Rowland (Ref. 5) shows that values as large as $d \simeq 2.5$ mm can occur, although somewhat smaller values are probably more characteristic for the ocean. In fact, Ball (Ref. 2) esti-mated $d \simeq 1.5$ mm from his experiments.

In order to compute the brightness temperature of a body of water with the temperature profile (B-1), it is also necessary to specify the dielectric constant of the water which, because of its temperature dependence, will likewise be a function of z. Equations expressing the dielectric constant as a function of temperature, water salinity and fre-quency have been developed by Stogryn (Ref. 7). With these results, the equations of Stogryn (Ref. 8) may be used to calculate the brightness temper-ature. Computations have been performed for a number of frequencies and angles of observation assuming that $d = 1.5$ mm. A parametric study of the brightness temperature as a function of δT showed that the brightness temperature change relative to that of a hypothetical body of water at the uniform temperature T_w is strictly proportional to δT in the range $-1.5 < \delta T < 1.5^{\circ}C$. Hence, the discussion of further results will be con-fined to the case $\delta T = 1^{\circ}C$ and be expressed in terms of the difference temperature

$$\Delta = T_u - T \qquad\qquad (B-2)$$

where T_u is the brightness temperature of the hypothetical uniform body of water with thermal temperature T_w and T is the brightness tempera-ture of the water with thermal profile (B-1). Of course, Δ is a function of angle, polarization, frequency, T_w, and water salinity.

Figure B-1 shows the variation of Δ, at a number of frequen-cies, with observation angle θ ($\theta = 0^{\circ}$ corresponds to a nadir-looking radiometer) for water with salinity $S = 35^{\circ}/oo$ and temperature $T_w = 15^{\circ}C$. The computations were carried out assuming a model atmosphere with a

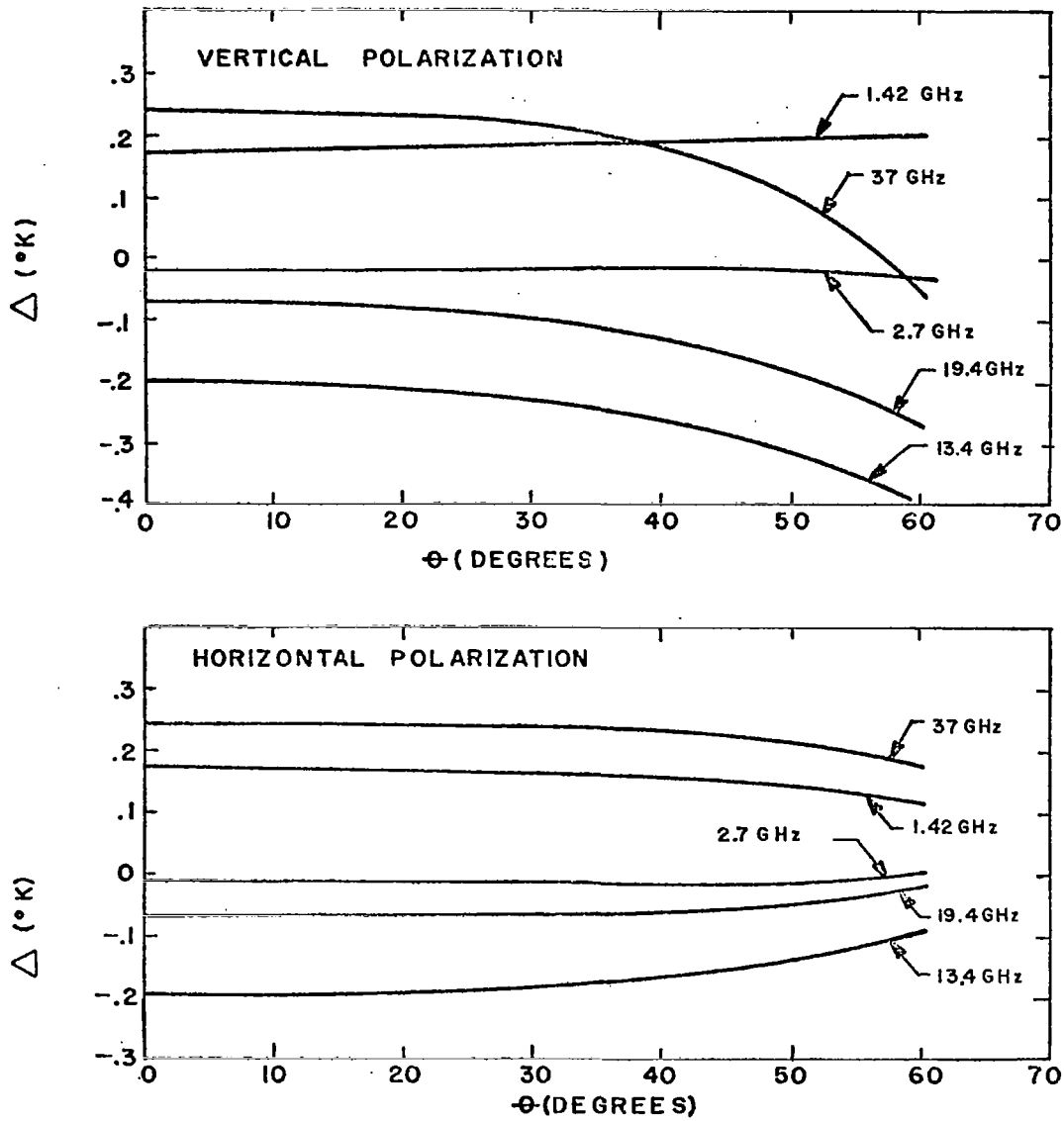Figure B-1. Δ as a Function of Angle for $T_w = 15^{\circ}C$ and $S = 35^{\circ}/oo$

moderate amount of water vapor and no clouds. However, Δ is rather insensitive to atmospheric conditions except in the extreme case of very heavy cloud cover and rain for the frequencies shown. It is evident that for both horizontal and vertical polarizations Δ is a slowly varying function of angle for $\theta < 40^{\circ}$ and that it is considerably smaller in magnitude than δT. Similar calculations for fresh water (S = $0^{\circ}/oo$) are shown in Figure B-2. The principal differences between fresh and sea water occur at frequencies below 13 GHz, as was to be expected.

It is also of interest to examine the dependence of Δ on T_w. In view of the above angular dependence which is exhibited in Figures B-1 and B-2, it is sufficient to consider only the cases $\theta = 0$ and $\theta = 50^{\circ}$. Figures B-3 and B-4 show results for water salinities of 35 and $0^{\circ}/oo$ respectively. In both cases, there is a substantial dependence on T_w. However, in no case does the magnitude of Δ exceed one half of δT.

Under the assumption that the brightness temperature at a given frequency could be considered to arise from a layer in the water at a definite temperature, McAlister (Refs. 3 and 4) has outlined a method for determining δT using a two-wavelength radiometer. While the computations presented here are based on a more detailed description of the effect of the thermal boundary layer on the brightness temperature and hence are described in a somewhat different form than given by McAlister, the basic technique suggested by him would provide a workable basis for determining δT provided that an adequate radiometer sensitivity could be achieved and that perturbations such as waves and whitecaps on the sea surface could be ignored. Further, because of the dependence on T_w indicated in Figures B-3 and B-4, the water temperature must be known with fair precision. Unfortunately, present evidence indicates that uncertainties in the microwave brightness temperature of the ocean due to changing surface conditions over a period of time and position (in the case of satellite-mounted instruments) will exceed the small changes due to the thermal boundary layer which are predicted by the present study. Hence a microwave radiometric experiment does not appear to be feasible.
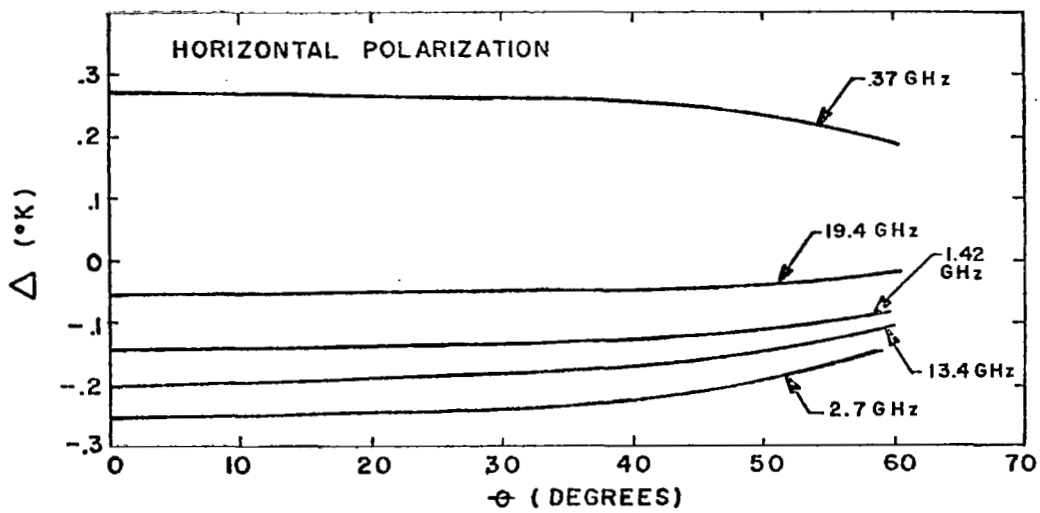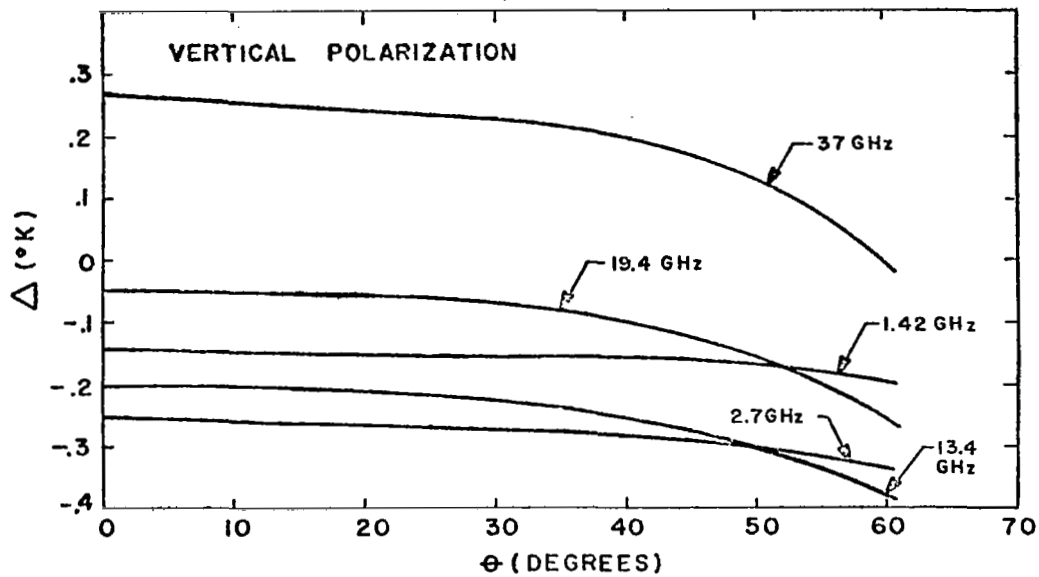
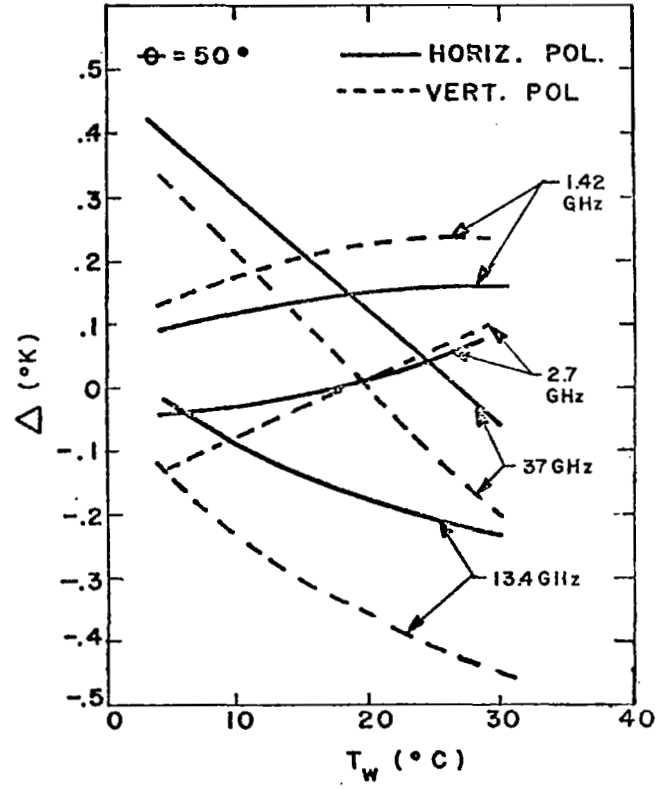Figure B-2. Δ as a Function of Angle for $T_w = 15^\circ C$ and $S = 0^\circ/oo$
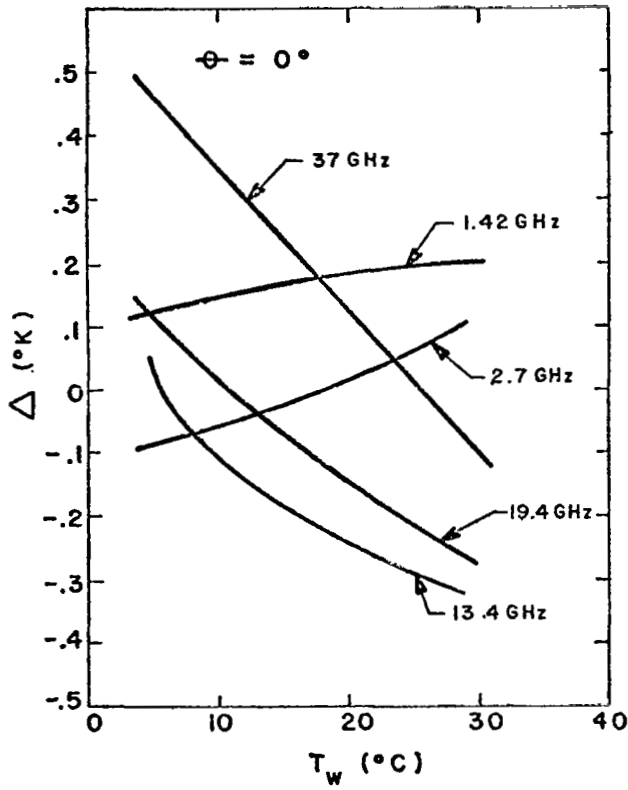
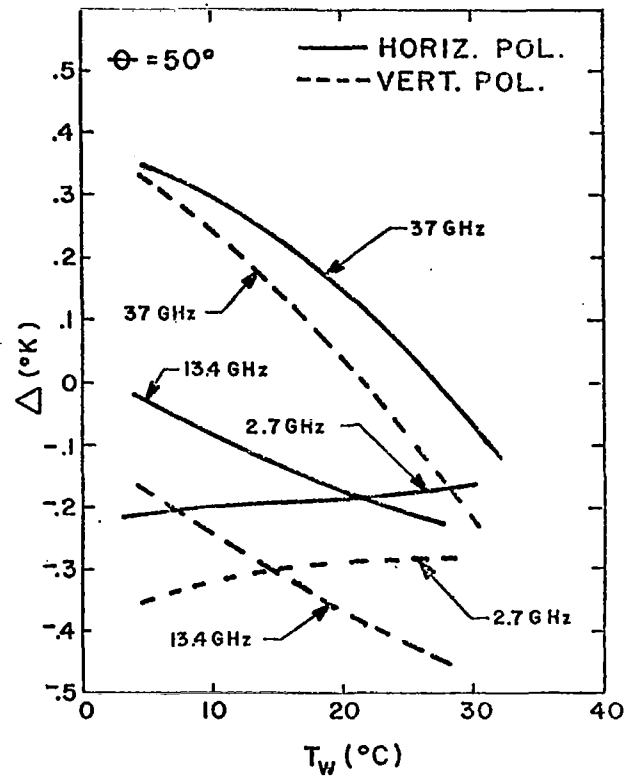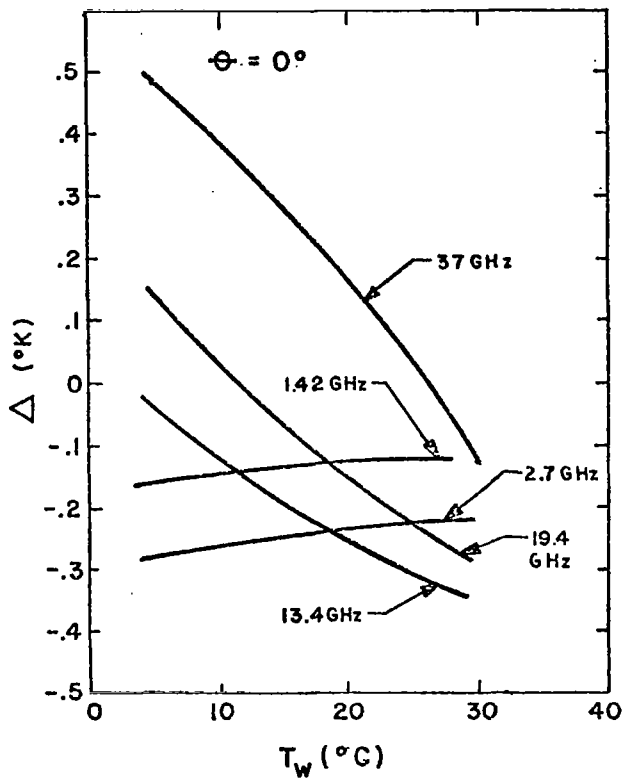Figure B-3. Δ as a Function of T_w for $S = 35^o/oo$

Figure B-4. Δ as a Function of T_w for $S = 0^{\circ}/oo$

REFERENCES

(1)   Ewing, G. and E. McAlister, "On the thermal boundary layer of the ocean," Science 131, 1374, 1960.

(2)   Ball, K., "Sea surface temperatures, "Australian J. Phys. 7, 649, 1954.

(3)   McAlister, E., "Infrared-optical techniques applied to oceanography," Applied Optics 3, 609, 1964.

(4)   McAlister, E., "A two-wavelength microwave radiometer for measurement of the total heat exchange at the air-sea interface," Applied Optics 4, 145, 1965.

(5)   Spangenberg, W. and W. Rowland, "Convective circulation in water induced by evaporative cooling," Physics of Fluids 4, 743, 1961.

(6)   Haüssler, W., "Über die temperature profile beiderseits einer verdunstenden wasseroberfläche," Wissenschaftliche Zeitschrift der Technischen Hochschule Dresden, 5, 435, 1956.

(7)   Stogryn, A., "Equations for calculating the dielectric constant of saline water at GHz frequencies, "IEEE Trans. Microwave Theory and Techniques, MTT, 19, 733, 1971.

(8)   Stogryn, A., "The brightness temperature of a vertically structured medium," Radio Science 5, 1397, 1970.